A Reference Multiparameter Viscosity Equation for R134a with an Optimized Functional Form

G. Scalabrin[a] **and P. Marchi**

Dipartimento di Fisica Tecnica, Università di Padova, via Venezia 1, I-35131 Padova, Italy

R. Span

Thermodynamik und Energietechnik (ThEt), Universität Paderborn, D-33098 Paderborn, Germany

(Received 21 December 2004; revised manuscript received 28 July 2005; accepted 29 August 2005; published online 19 May 2006)

An optimization technique was applied to develop a functional form for a multiparameter viscosity equation $\eta = \eta(\rho, T)$ for R134a. The results obtained are very promising, with an average absolute deviation of 0.55% for the currently available 549 primary data points. Compared to viscosity equations available in the literature, this is a significant improvement. Advantages become evident especially at gaseous states. As usual, both the development and the use of the viscosity equation require a highly accurate equation of state in order to convert the independent variables used for the experimental data and in most applications, (P,T), into the independent variables of the viscosity equation, (ρ,T). Though the equation was developed directly using the available data, the zero-density viscosity and the reduced second viscosity virial coefficient are correctly reproduced in the data range. The technique used to develop the equation, which is heuristic and not theoretically founded, is capable of selecting consistent data sets and thus is a powerful tool for screening the available experimental data. For the viscosity surface representation of a pure fluid this study shows that the limit in the achievement of a better accuracy is much more due to the present experimental uncertainty level for this property rather than to the effectiveness of the proposed modeling method. © *2006 American Institute of Physics.* [DOI: 10.1063/1.2141635]

Key words: R134a, transport properties correlation techniques; viscosity; multiparameter equations; 1,1,1,2-tetrafluoroethane.

Contents

List of Tables

[a]Author to whom correspondence should be addressed; electronic mail: gscala@unipd.it

List of Figures

1. Introduction

The halofluorocarbon R134a (1,1,1,2-tetrafluoroethane) is a refrigerant with a wide application range, whose utilization has greatly increased in recent years. Both the thermodynamic and the transport properties of this fluid are of great interest due to its important engineering applications.

Two different approaches are found in the literature for the representation of the viscosity surface of a fluid. The first approach includes predictive or semipredictive models which are often based on corresponding states theory.[1–10] In many cases these models are capable of predicting the viscosity with an accuracy level sufficient for engineering calculations. Theoretically based models, for instance those including the evaluation of collision integrals, have also been developed. Even if they do not require experimental data, in some cases they are not yet accurate enough to yield a reference equation for viscosity.

The second approach can be either semitheoretically founded or totally heuristic; for both these groups suitable models have been developed. The first group includes the widely used state-of-the-art technique for the development of viscosity equations, which is based on the residual concept superimposing three parts: the dilute-gas term, the excess term, and the critical enhancement term.[11] This technique usually leads to an equation in the form $\eta = \eta(\rho,T)$ and it is in some extent correlative requiring experimental data as evenly distributed as possible over the whole $\eta\rho T$ surface. Equations of this type will be referred to as "conventional equations" in this paper. Since viscosity data are inevitably related to the experimentally accessible variables (T,P), an equation of state is needed to convert (T,P) into (T,ρ). Moreover, viscosity data at low pressures have to be extrapolated to zero pressure to fit the coefficients of the dilute-gas term in the viscosity equation.

In more detail it can then be pointed out that:

(1) Though the structure of the conventional viscosity equation sounds theoretically well based, experimental data distributed over the whole $\eta\rho T$ surface are needed to regress the coefficients of the three contributions;
(2) It is by no means easy to find the most suitable analytical form for representing the density dependence of the excess term;
(3) The fitting procedure is not direct from the data, because each value has to be split into the three contributions terms with separate correlation of each of them; and
(4) A highly accurate equation of state is needed for converting the measured variables (T,P) into (T,ρ). This is unavoidable for all kinds of viscosity equations covering the whole fluid surface, unless implicit functional forms are used.[12]

However, considering that experimental data covering the whole $\eta\rho T$ surface are needed for the development of a conventional viscosity equation dedicated to a target fluid, one could try to test a single correlative technique directly based on all the available data. The analytical form of the new model has to be highly flexible in fitting the experimental viscosity surface of a generic fluid, but at the same time intercorrelations between different terms in the equation should be minimized for numerical reasons. To fulfill this requirement, a number of totally correlative methods, composing the second group of models pertaining to the cited second approach, has been developed. These methods are based either on the multilayer feedforward neural networks[13–17] or on a combination of the extended corresponding states and the neural networks techniques.[18,19]

A very effective correlation technique was searched to supply an accurate viscosity equation describing the whole range of fluid states. In this work a functional form to represent the viscosity surface of R134a with high accuracy and with the widest range of validity, but totally based on experimental data as an alternative to a conventional viscosity equation, was studied. Some tests have shown that the technique for optimizing the functional form of multiparameter equations of state set up by Setzmann and Wagner[20] and applied mainly in the development of accurate fundamental equations of state has the required characteristics, and that this technique can be applied to experimental data sets for the viscosity of a fluid as well.

A new correlation technique is then proposed here, based on the Setzmann and Wagner method.[20] The main aspect of this paper is the application of this correlation method to the viscosity data available for R134a and the development of a multiparameter viscosity equation.

2. Procedure for Developing an Empirical Equation for Viscosity

2.1. Fitting a Multiparameter Empirical Equation

The viscosity surface of a fluid can be written through an empirical equation in the form $\eta(T,\rho,\bar{n})$ with $\bar{n}$ representing the vector of the individual coefficients to be fitted.

The optimum set of coefficients $\bar{n}$ for the empirical equation is obtained by minimizing an objective function composed of a sum of squares as follows:

$$\chi^2(\bar{n}) = \sum_{i=1}^{N} \left(\frac{\eta_{\mathrm{exp}} - \eta_{\mathrm{calc}}(\bar{n})}{\eta_{\mathrm{exp}}} \right)_i^2, \qquad (1)$$

where N is the total number of primary experimental points and the subscripts calc and exp stand for calculated and experimental values, respectively.

TABLE 1. Substance specific parameters for the target fluid R134a

		Reference
M (kg mol^{-1})	0.102032	21
T_c (K)	374.18	21
P_c (MPa)	4.05629	21
ρ_c (kg m^{-3})	508.0	21
H_c (μPa s)	25.17975	—

TABLE 2. Summary of the available viscosity data sets for R134a

Reference	First author	Phase[a]	NPT	T range (K)	P range (MPa)	Measurement method[b]	Class
			Liquid				
24	Assael	*l*	32	273–333	1.0–14.6	VW	II
25	Diller	*l*	63	200–300	0.6–33.7	TC	II
26	Okubo	*l*	73	213–373	1.6–30.2	CV	I
27	Oliveira	*l*	43	293–343	0.7–51	VW	I
27	Oliveira	*l*	11	238–289	0.1–0.8	VW	I
28	Padua	*l*	37	248–298	0.7–100.1	VW	II
29	Ruvinskij	*l*	23	258–361	0.3–6.4	CV	I
24	Assael	*sl*	7	273–333	*	VW	II
25	Diller	*sl*	30	175–320	*	TC	II
30	Han	*sl*	21	233–333	*	CV	II
31	Heide	*sl*	14	223–353	*	RB	I
32	Kumagai	*sl*	8	273–343	*	CV	II
33	Laesecke	*sl*	91	241–350	*	OD	I
27	Oliveira	*sl*	17	238–343	*	VW	I
34	Padua	*sl*	5	198–298	*	VW	II
35	Ripple	*sl*	14	250–306	*	CV	II
36	Sagaidakova	*sl*	18	203–373	*	C	II
37	Shankland	*sl*	12	251–343	*	CV	II
	Total		519				
			Vapor				
38	Assael	*v*	22	274–333	0.1–1.5	VW	I
39	Dowdell	*v*	6	308–403	0.1	CV	I
40	Mayinger	*v*	311	253–483	0.1–4.0	OD	II
41	Nabizadeh	*v*	35	303–424	0.1–4.0	OD	II
42	Pasekov	*v*	37	275–371	0.3–0.6	CV	I
29	Ruvinskij	*v*	6	382–405	0.7–3.4	CV	II
43	Schramm	*v*	10	250–600	0.1	C	II
44	Shibasaki	*v*	113	298–423	0.1–3.9	OD	I
45	Wilhelm	*v*	71	297–438	0–0.3	TC	I
38	Assael	*sv*	7	273–333	*	C	I
40	Mayinger	*sv*	22	247–353	*	OD	II
46	Oliveira	*sv*	14	243–343	*	VW	II
	Total		654				
			Supercritical				
40	Mayinger	*sc*	65	383–483	4.5–11.0	OD	II
41	Nabizadeh	*sc*	6	423–424	4.5–6.4	OD	II
26	Okubo	*sc*	8	423	10.1–29.8	CV	I
29	Ruvinskij	*sc*	5	382–405	4.2–6.2	CV	II
44	Shibasaki	*sc*	13	398–423	4.2–5.6	OD	I
	Total		97				
			Overall				
	Overall		1270				

[a]Phase: *l* = liquid, *sl* = saturated liquid, *v* = vapor, *sv* = saturated vapor, and *sc* = supercritical.
[b]Measurement method: C = calculated, CV = capillary viscometer, OD = oscillating disk viscometer, RB = rolling ball viscometer, TC = torsional crystal viscometer, and VW = vibrating wire viscometer.

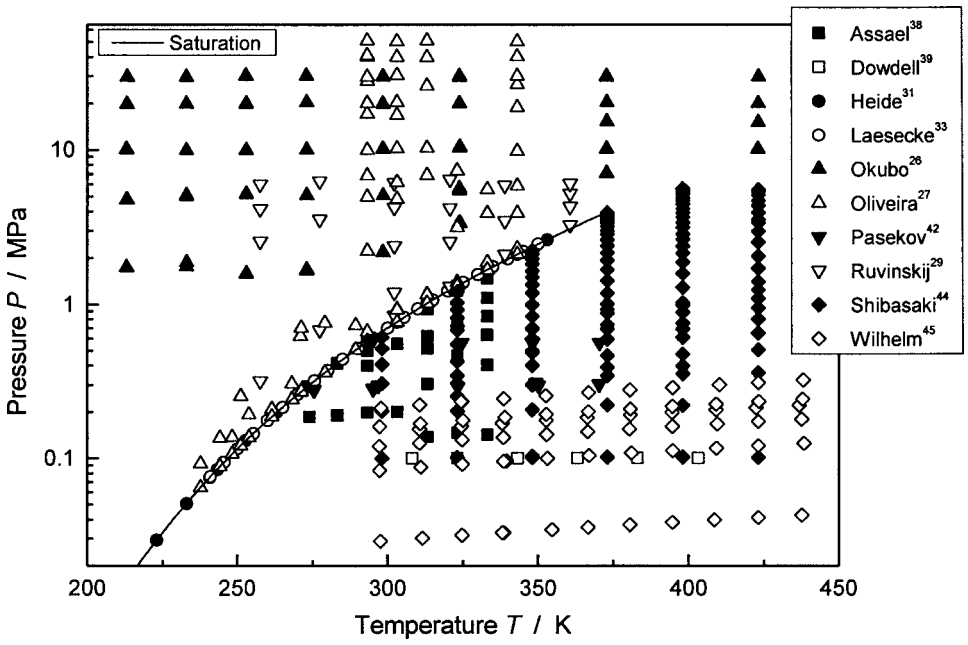

FIG. 1. Distribution of the data selected as primary data.

The algorithm developed by Setzmann and Wagner[20] constitutes the minimization technique used for the present study. Given a bank of terms the algorithm determines the functional form which yields the best representation of the selected experimental data.

2.2. Bank of Terms

For the optimization of the functional form a bank of terms composed of a total of 267 terms is used and this can be written as

$$\eta_r = \sum_{i=0}^{10} \sum_{j=0}^{20} n_{ij} T_r^i \rho_r^j + \sum_{i=0}^{5} \sum_{j=0}^{5} n_{ij} T_r^i \rho_r^j e^{-2\rho_r^2} \qquad (2)$$

where

$$T_r = T/T_c$$

$$\rho_r = \rho/\rho_c \qquad (3)$$

$$\eta_r = \ln(\eta/H_c + 1)$$

$$H_c = \frac{M^{1/2} P_c^{2/3}}{R^{1/6} N_A^{1/3} T_c^{1/6}}.$$

For the target fluid R134a the parameters involved in the former variable definitions are reported in Table 1.

Further parameters are the molar gas constant, $R = 8.314472\ \mathrm{J\,mol^{-1}\,K^{-1}}$, assumed from Mohr and Taylor,[22] and the Avogadro number, $N_A = 6.0221353 \times 10^{23}\ \mathrm{mol^{-1}}$, assumed from Becker *et al.*[23]

3. Multiparameter Viscosity Equation for the Whole Surface

3.1. Experimental Data

For R134a the viscosity data sets available from the literature are presented in Table 2. The significance of the column "Class" will be explained in Sec. 3.2.

3.2. Screening Procedure and Primary Data Sets

The screening of the experimental data available from the literature has been performed according to the following procedure.

Because a viscosity equation in the conventional format for R134a was made available by Krauss *et al.*[11] this was used to screen the data within the validity range of the equation. All the available data sets were considered, including those not assumed for the conventional equation development since they were published afterwards. An error threshold with respect to this equation was conventionally selected at an average absolute deviation (AAD) of 5%. Each data set was evaluated as a whole, because it was supposed that all the data from each set were obtained with a homogeneous accuracy. The data sets from this first screening compose the preliminary sources. The preliminary data are obtained including the points of the preliminary sources which are outside the validity range of the conventional viscosity equation.

A first regression with the optimization algorithm was based on this set of preliminary data. A first selection of primary data sets was obtained considering only data with a threshold of 2%–3% for the AAD and a low value of the bias. A further screening of these data was carried out through regressions with the optimization algorithm refining the choice of the so called primary data sets. During this

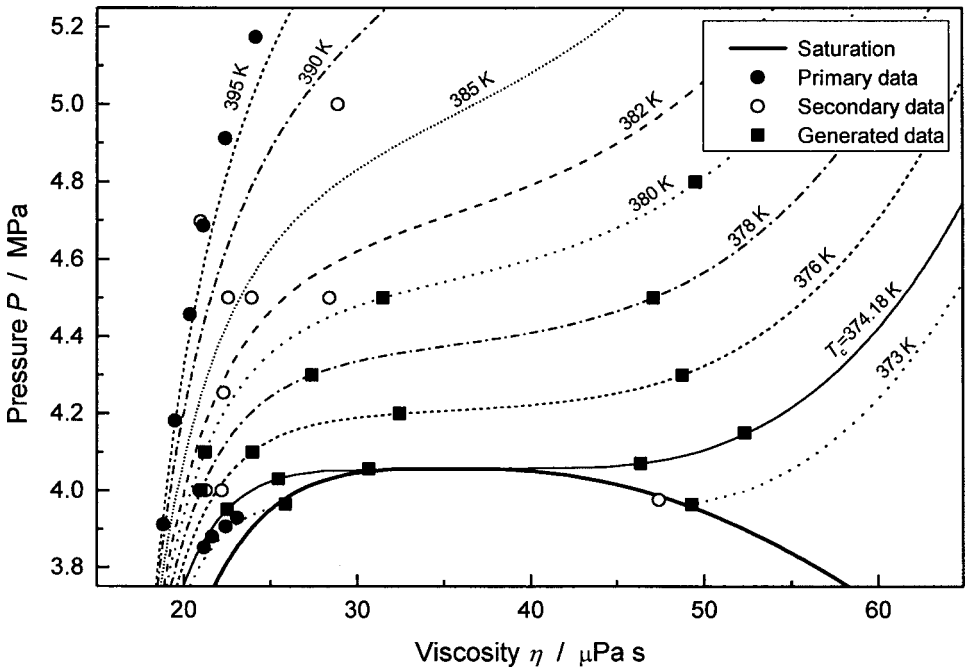

FIG. 2. Representation of experimental and generated data in the near critical region.

procedure some sets were moved from primary to secondary, and vice versa, searching for AAD values of the single sets to be as similar as possible to the overall value for the primary data and for the bias values close to zero.

The aim of the procedure was to gather sets with the lowest error deviations and statistically centered as much as possible with respect to the multiparameter viscosity equation. This screening finally led to a stable selection of primary data on which the final version of the multiparameter equation was regressed. In Table 2 and in the following tables the column ''Class'' reports the sets classification: the primary data sets are marked with the symbol I, whereas the secondary data are marked with II. The distribution of the primary data on the P,T plane is shown in Fig. 1.

TABLE 3. Near critical data generated by the conventional equation of Krauss *et al.*[11]

T (K)	P (MPa)	η (μPa s)
373.00	3.9633	49.259
373.00	3.9633	25.881
374.18	3.9500	22.517
374.18	4.0300	25.458
374.18	4.0563	30.676
374.18	4.0700	46.339
374.18	4.1500	52.312
376.00	4.1000	23.979
376.00	4.2000	49.259
376.00	4.3000	25.881
378.00	4.0000	22.517
378.00	4.3000	25.458
378.00	4.5000	30.676
380.00	4.1000	46.339
380.00	4.5000	52.312
380.00	4.8000	23.979

3.3. Near Critical Region

A very limited number of experimental points is available for R134a in the near critical region and this causes a lack of information about the trend of the viscosity surface in the region where a strong variation of the viscosity derivatives with respect to the independent variables is expected. For the heuristic modeling procedure used here, it was assumed that a certain number of points with a rather regular distribution in that region is needed to let the new equation follow the characteristic trend close to the critical region.

To overcome this difficulty, data have been generated by the conventional viscosity equation for R134a,[11] including a critical enhancement following the Olchowy and Sengers theory,[47,48] for a total of 16 points distributed as shown in Fig. 2, see Table 3. The isotherms and the saturation curve are from the conventional equation.[11] These data have been used as primary data for the regression of the new viscosity multiparameter equation. The goal of this integration is only to obtain a correct trend but not to assure a documented accuracy for the equation in the near critical region.

TABLE 4. Parameters of Eq. (4)

i	g_i	h_i	n_i
1	0.0	2.0	0.6564868
2	0.0	20.0	0.6882417×10^{-10}
3	1.0	0.0	0.5668165
4	1.0	3.0	−0.2989820
5	2.0	0.0	−0.1061795
6	2.0	4.0	0.6245080×10^{-1}
7	4.0	14.0	0.2758366×10^{-6}
8	0.0	1.0	−0.1621088
9	2.0	1.0	0.1675102
10	5.0	3.0	-0.9224693×10^{-1}

TABLE 5. Validity limits of Eq. (4)

T (K)	210–450
P (MPa)	⩽55

The influence of the critical enhancement for viscosity is limited to a very narrow region centered on the critical point where the viscosity approaches an infinite limit.[49] In this work the modeling of a critical enhancement has been omitted similarly to the majority of the literature dedicated to viscosity equations.

TABLE 6. Deviations of the new viscosity equation, Eq. (4), with respect to primary, secondary, and overall data in the liquid, vapor, and supercritical regions. Data are within the Eq. (4) validity limits

Reference	First author	Phase	NPT	T range (K)	P range (MPa)	Measurement method	AAD (%)	Bias (%)	MAD (%)	Class
					Liquid					
26	Okubo	*l*	73	213–373	1.6–30.2	CV	0.66	−0.52	2.12	I
27	Oliveira	*l*	54	238–343	0.1–51.0	VW	1.14	0.93	2.91	I
29	Ruvinskij	*l*	23	258–361	0.3–6.4	CV	1.14	−0.98	2.66	I
31	Heide	*sl*	14	223–353	*	RB	1.23	−0.73	3.05	I
33	Laesecke	*sl*	91	241–350	*	OD	0.67	0.05	1.96	I
27	Oliveira	*sl*	17	238–343	*	VW	0.96	0.72	2.08	I
	Primary		272				0.85	−0.01	—	
24	Assael	*l*	32	273–333	1.0–14.6	VW	2.19	2.19	2.77	II
25	Diller	*l*	55	220–300	0.6–33.7	TC	5.86	5.86	10.15	II
28	Padua	*l*	28	248–298	0.7–45.1	VW	3.45	3.45	5.78	II
24	Assael	*sl*	7	273–333	*	VW	1.92	1.92	2.09	II
25	Diller	*sl*	23	210–320	*	TC	6.70	6.70	8.84	II
30	Han	*sl*	21	233–333	*	CV	2.15	1.60	6.41	II
32	Kumagai	*sl*	8	273–343	*	CV	4.16	4.16	10.66	II
34	Padua	*sl*	4	223–298	*	VW	7.03	7.03	14.68	II
35	Ripple	*sl*	14	250–306	*	CV	3.15	3.15	5.93	II
36	Sagaidakova	*sl*	17	213–373	*	C	2.98	−2.98	4.53	II
37	Shankland	*sl*	12	251–343	*	CV	8.20	8.20	23.51	II
	Total		493				2.41	1.70	—	
					Vapor					
38	Assael	*v*	22	274–333	0.1–1.5	VW	0.67	−0.25	2.59	I
39	Dowdell	*v*	6	308–403	0.1	CV	0.48	0.13	0.65	I
42	Pasekov	*v*	37	275–371	0.3–0.6	CV	0.30	−0.05	1.39	I
44	Shibasaki	*v*	113	298–423	0.1–3.9	OD	0.19	0.00	0.77	I
45	Wilhelm	*v*	71	297–438	0–0.3	TC	0.08	0.04	0.33	I
38	Assael	*sv*	7	273–333	*	C	0.79	0.23	1.84	I
	Primary		256				0.24	−0.01	—	
40	Mayinger	*v*	239	253–443	0.1–4.0	OD	3.32	3.32	11.08	II
41	Nabizadeh	*v*	35	303–424	0.1–4.0	OD	3.80	3.80	12.64	II
29	Ruvinskij	*v*	6	382–405	0.7–3.4	CV	1.55	−1.28	3.04	II
43	Schramm	*v*	7	250–424	0.1	C	1.05	1.00	2.58	II
40	Mayinger	*sv*	22	247–353	*	OD	3.26	3.09	10.62	II
46	Oliveira	*sv*	14	243–343	*	VW	4.25	4.25	7.85	II
	Total		579				1.96	1.82	—	
					Supercritical					
26	Okubo	*sc*	8	423	10.1–29.8	CV	0.93	0.39	1.27	I
44	Shibasaki	*sc*	13	398–423	4.2–5.6	OD	0.24	−0.06	0.59	I
	Primary		21				0.51	0.11	—	
40	Mayinger	*sc*	30	383–443	4.5–9.0	OD	11.34	11.34	15.14	II
41	Nabizadeh	*sc*	6	423–424	4.5–6.4	OD	11.14	11.14	12.96	II
29	Ruvinskij	*sc*	5	382–405	4.2–6.2	CV	1.59	1.59	2.30	II
	Total		62				6.86	6.73	—	
					Generated data					
Near critical generated data			16				0.83	0.22	2.18	
					Overall					
Overall primary			549				0.55	−0.01	—	
Overall			1134				2.42	2.04	—	

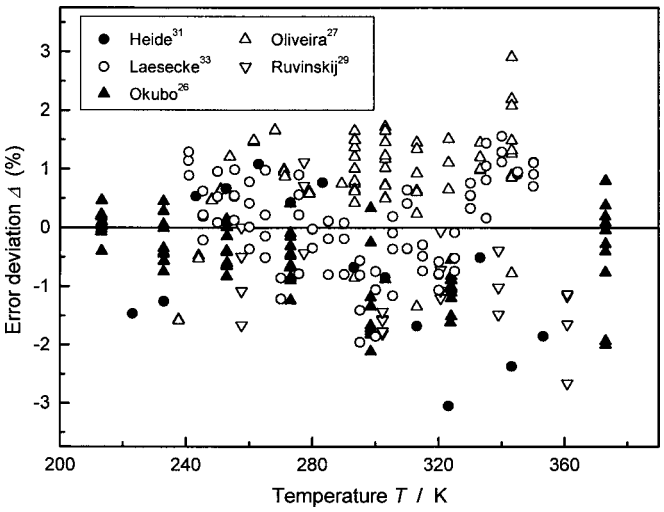

FIG. 3. Deviations between primary experimental data in the liquid phase and values calculated from Eq. (4).

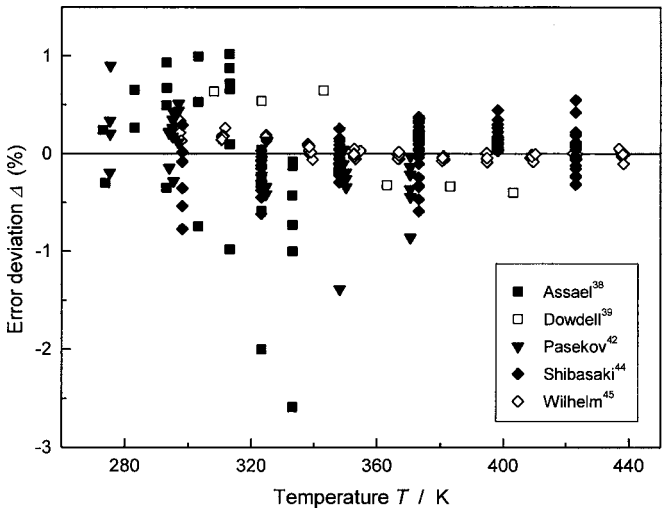

FIG. 4. Deviations between primary experimental data in the vapor phase and values calculated from Eq. (4).

3.4. The New Equation for the Viscosity of R134a

Once the final choice of the primary data sets was made, an equation in the form $\eta = \eta(\rho, T)$ was obtained from the optimization procedure. This equation reads:

$$\eta_r = \sum_{i=1}^{7} n_i T_r^{g_i} \rho_r^{h_i} + e^{-2\rho_r^2} \sum_{i=8}^{10} n_i T_r^{g_i} \rho_r^{h_i}. \tag{4}$$

The coefficients and exponents of Eq. (4) are reported in Table 4.

The validity limits of Eq. (4) are reported in Table 5. The extrapolation of the equation outside these validity limits, particularly at low temperatures and at high pressures, should be avoided since it may result in rather unreliable values.

As shown in Fig. 1, the primary data do not regularly fill all the regions of the stated validity range, but we chose not to assume an irregular contour for the validity range itself. This assumption will be discussed further on in Sec. 5.3.

Because a conversion from (T, P) to (T, ρ) is needed for a viscosity equation in the form $\eta(T, \rho)$, the R134a dedicated equation of state (DEoS) of Tillner-Roth and Baehr[21] was used to transform the data.

4. Validation of the New Viscosity Equation

The new equation has been validated in detail with respect to both primary and secondary data; the results are reported in the present section.

The deviations with respect to primary data and to the data generated in the near critical region, Table 6 and Figs. 3–5, are considered as remaining deviations of the regression because the equation was regressed on these data. All other data were not considered in the regression.

Through all the present work the error deviation Δ has been calculated as:

$$\Delta = \frac{\eta_{\text{exp}} - \eta_{\text{calc}}}{\eta_{\text{exp}}} \tag{5}$$

where exp and calc stand for experimental and calculated values, respectively.

From the error deviations Δ the following statistical quantities are evaluated: the average absolute deviation (AAD %), the bias (bias %), and the maximum absolute deviation (MAD %). These are calculated as:

$$\text{AAD\%} = \frac{100}{\text{NPT}} \sum_{i=1}^{\text{NPT}} |\Delta|_i$$

$$\text{Bias\%} = \frac{100}{\text{NPT}} \sum_{i=1}^{\text{NPT}} (\Delta)_i \tag{6}$$

$$\text{MAD\%} = 100 \ \ \text{Max}|\Delta|_i .$$

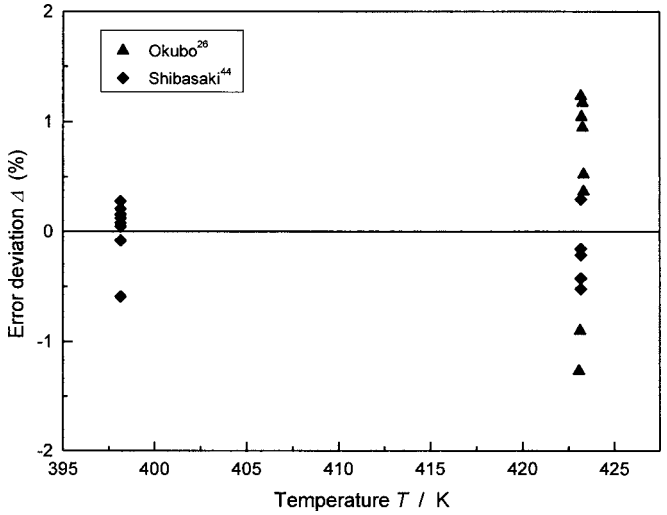

FIG. 5. Deviations between primary experimental data in the supercritical region and values calculated from Eq. (4).

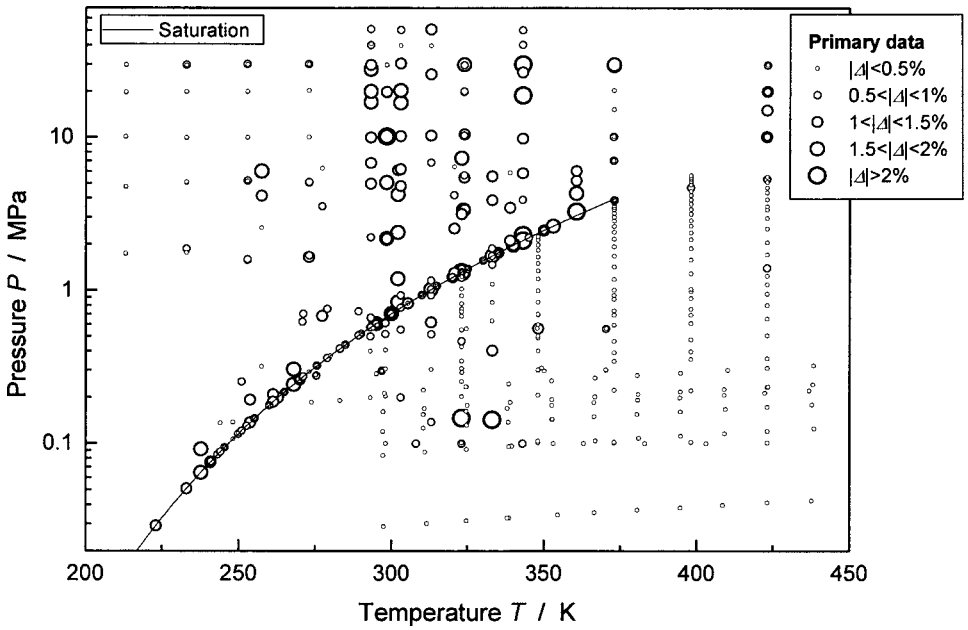

FIG. 6. Deviations between all primary experimental data and values calculated from Eq. (4) shown in a P,T diagram. The size of the symbols indicates the deviation between the selected experimental data and corresponding values calculated from Eq. (4).

In Fig. 6 the deviations between the new viscosity equation and the primary data, indicated by the size of the symbols, are shown in a P,T diagram. This plot shows the high precision of the new equation especially with respect to the gas-phase viscosities. Furthermore, in Fig. 7 the deviations between Eq. (4) and all the primary experimental data are shown as a function of pressure for several steps of temperature. The lines represent values calculated from the two conventional equations, from Krauss *et al.*[11] and from Huber *et al.*[50] For each figure the temperature of the comparison with the two equations was taken at the mean value of the indicated range.

The Huber *et al.*[50] equation is very concisely presented with a quite short discussion about the experimental sources used for the correlations of the equation and also the validation with respect to the different regions is largely lacking in terms of a detailed statistical analysis. Consequently, the Krauss *et al.*[11] equation is the present reference for this fluid, whereas the Huber *et al.*[50] equation is considered for comparison but with lower evidence with respect to the Krauss one.

5. Behavior of the Viscosity Surface

5.1. Representation of the Viscosity Surface on a T,η Plane

Isobars in the gas phase and the vapor side of the saturation curve obtained from the new viscosity equation are plotted on a T,η plane in Fig. 8. A line of viscosity minima is observed in the dense gas region. Numerical information on the locus of such viscosity minima is reported in Table 7.

As it can be seen from Fig. 8, the viscosity minima are found in the pressure range $2.38 \leqslant P/\mathrm{MPa} \leqslant 6.0$ corresponding to $0.587 \leqslant P_r \leqslant 1.480$. At higher pressures the minimum is shifted to temperatures beyond the temperature range where Eq. (4) is valid. The locus of the minima can be represented up to 6 MPa by a function in the form:

$$y = a + bx + cx^2, \tag{7}$$

which variables and corresponding parameters are reported in Table 8.

5.2. Representation of the Viscosity Surface on a P,η Plane

Figure 9 shows the plot of isotherms calculated from Eq. (4) on a P,η plane. In Fig. 10 a magnified part in the region of vapor close to the critical point is shown. The shape of the surface is reasonable and the trend of isotherms close to the critical one is correct, under the hypothesis of neglecting a very narrow range centered at the critical point where the viscosity critical enhancement contribution is really significant.

Figure 11 shows isotherms calculated from the new viscosity equation on a P,η plane in the region of low density vapor. Again, a line of viscosity minima is found in the graphical representation. Numerical values for the location of the minima are given in Table 9. The same line of viscosity minima is also found when plotting isotherms on a η,ρ plane (see Fig. 13).

The comparison between experimental values and values calculated from Eq. (4) indicates that the new equation is very accurate in the low-density gas region (see Table 10). Thus, the reported minima are considered reliable.

As shown in Fig. 11 a locus of minima is present in the temperature range $289 \leqslant T/\mathrm{K} \leqslant 368$, that is $0.772 \leqslant T_r \leqslant 0.983$. Using the coefficients and the variable assignment given in Table 11, the locus of the minima can be described by Eq. (7) again.

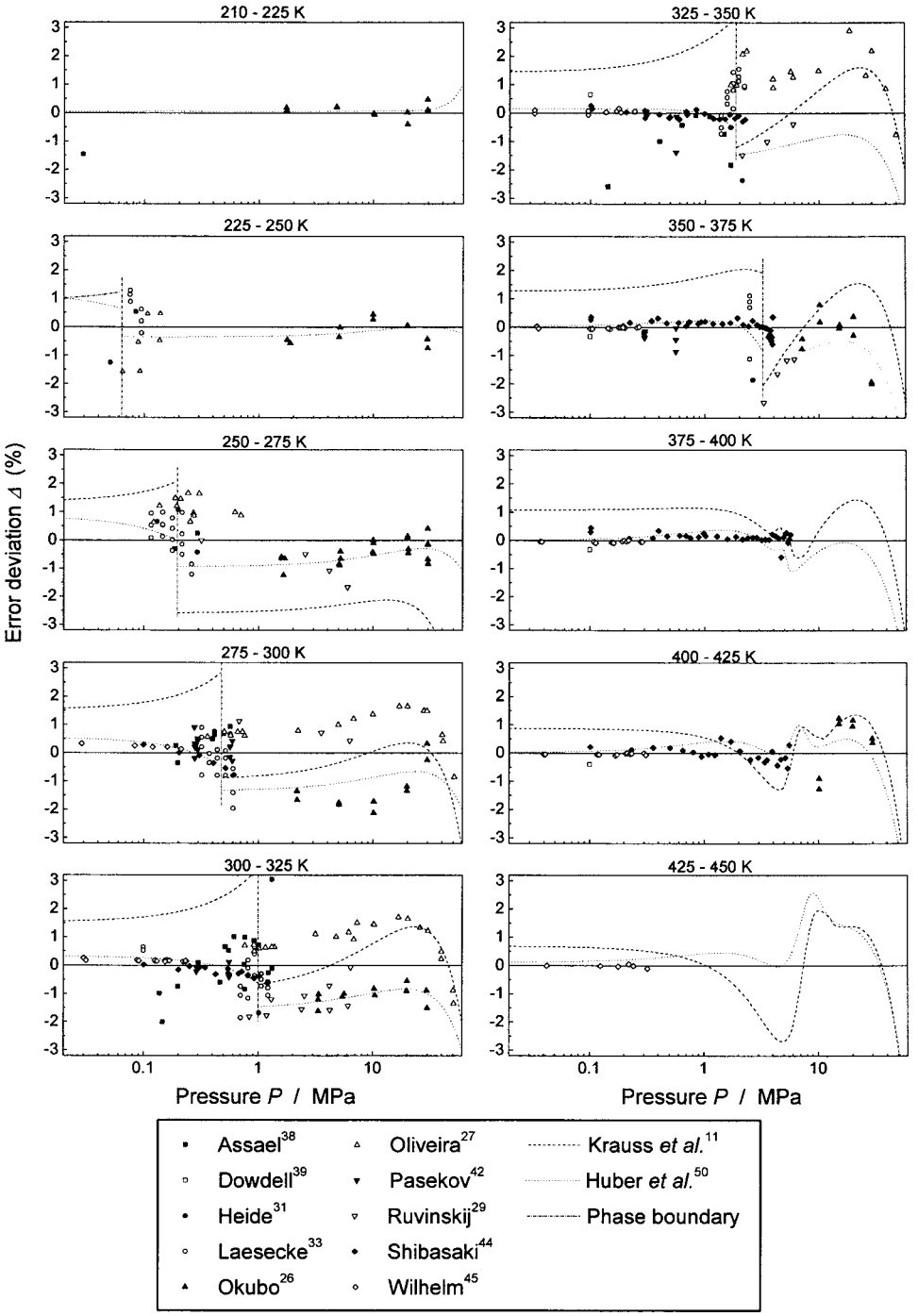

FIG. 7. Deviations between all experimental points in the primary data sets and Eq. (4), sorted by temperature. The plotted lines correspond to values calculated from the conventional equations by Krauss *et al.*[11] and Huber *et al.*[50]

5.3. Discussion on the Validity Limits

The validity limits of the new viscosity Eq. (4) were briefly discussed in Sec. 3.4. However, the preceding plots show that the primary data do not uniformly fill a single regular range, both in temperature and in pressure. For the sake of precision, an irregular contour for the validity range should be selected. But, looking in particular at Figs. 9 and 11, it is evident that the trends of the new equation in the areas where experimental points are not available are regular and that they correspond to the expected behavior. This indicates that the equation can be used in these areas as well, assuming that the accuracy of the equation cannot be verified in these areas due to a lack of experimental data. In fact in Fig. 9 one can see for instance a total lack of data for liquid states at $T<290$ K and $P>30$ MPa. Figure 11 shows that data are not available at $T<270$ K for vapor states as well. However, at low temperatures gas densities are small enough to extrapolate to the zero density limit, assuming that the extrapolation behavior is reasonable (see Sec. 7). At liquid states, the change from 30 to 55 MPa hardly increases the density of the fluid and thus the independent variable of the equation, the density, is hardly extrapolated.

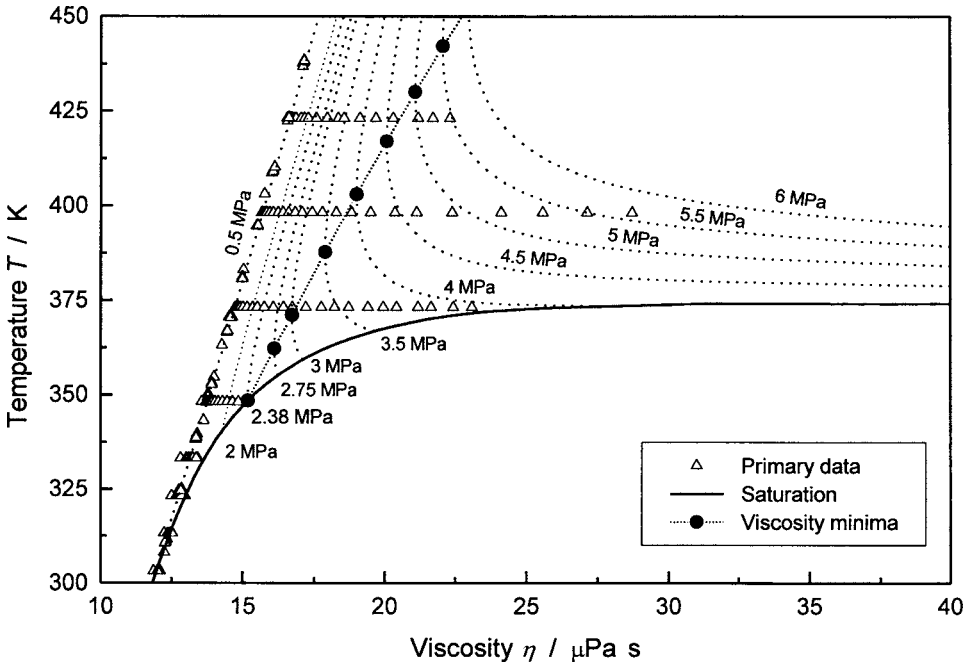

FIG. 8. Isobars and saturated-vapor line calculated from Eq. (4) and plotted in a T, η plane. Viscosity minima are found in the dense gas phase.

Slightly increased uncertainties occur when the equation is applied in areas within the limits of the range of validity given in Table 5 where there are no primary data available for comparisons.

6. Comparison with the Conventional Equations

Two conventional viscosity equations are presently found in the literature. The equation by Krauss *et al.*[11] is commonly considered the standard for the viscosity of R134a and is used for comparison throughout this paper. The density used in this equation has to be calculated by the DEoS from Huber and McLinden[51] as in the original publication. The comparison is made within the validity limits of this equation, which are more narrow with respect to the other equations considered.

With respect to the primary data the new Eq. (4) is largely superior to the conventional equation from Krauss *et al.*[11] for both the single phase regions and the whole surface, as the AAD and bias values show in Table 12. A large difference is found for the vapor primary data: the present equation has an excellent behavior but the conventional one is shifted with respect to the data. In the region of low-density vapor the conventional equation performance with respect to the present data base is shown in Fig. 12 and this figure has to be compared with the former Fig. 11. For the conventional equation development a reduced number of data, with worse experimental quality, was available and consequently the accuracy of that equation with respect to the present data base is considerably lower.

The equation by Huber *et al.*[50] is also compared in Table 12 to the primary data set considered in this work. In the vapor and supercritical regions such an equation performs better than the equation by Krauss *et al.*,[11] but it is slightly worse in the liquid. Compared to the new equation, Eq. (4), the equation by Huber *et al.* shows a comparable accuracy for the vapor and supercritical regions, whereas it has a lower performance in the liquid.

TABLE 7. Locus of the minima of the viscosity surface as calculated from Eq. (4) inside its range of validity

P (MPa)	$T_{\min}$ (K)	$\eta_{\min}$ (μPa s)
2.38	348.46	15.191
2.75	362.49	16.112
3.00	371.41	16.713
3.50	388.12	17.864
4.00	403.46	18.949
4.50	417.63	19.971
5.00	430.77	20.930
5.50	443.04	21.829
6.00	454.57	22.668

7. Zero-Density Limit and Initial Density Dependence of the New Viscosity Equation

In the literature some semitheoretical analyses of the viscosity of the low density vapor region are presented.[53–55] A

TABLE 8. Variables and parameters of Eq. (7) for the locus of the viscosity minima found along isobars

x	y	a	b	c
P_r	T_r	0.660341	0.522214	−0.100007
P_r	ρ_r	0.105012	0.307714	−0.0563159
P_r	η_r	0.304670	0.324201	−0.0651411

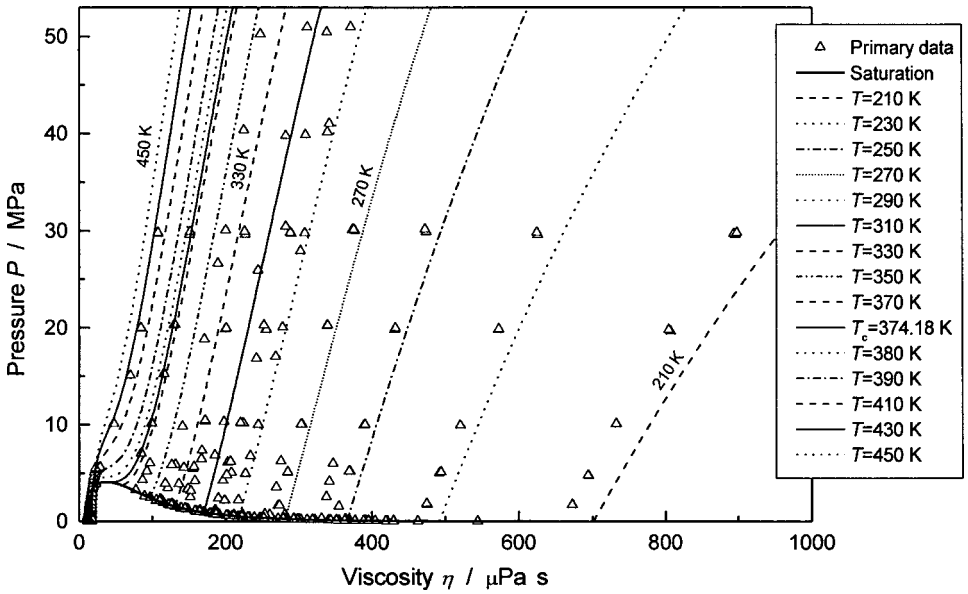

FIG. 9. Isotherms and saturation curve calculated from Eq. (4) on a P,η plane.

comparison with those models is the aim of the present section. To allow for a comparison on this level, both the new equation and the available experimental data have to be reduced to the format used in the corresponding literature.

The available primary experimental data in the vapor region and the viscosity along some isotherms and along the saturation line calculated from the multiparameter viscosity equation, Eq. (4), are represented in Fig. 13. A total of 229 primary points is available in the selected range, which is defined by $230 \leqslant T/\mathrm{K} \leqslant 450$ and $\rho \leqslant 100\ \mathrm{kg\,m^{-3}}$. For these data, Eq. (4) yields very low average deviations, namely AAD=0.25%, bias=0.00%, and MAD=2.59%. The locus of the viscosity minima on the isotherms is shown as well.

The viscosity predicted by an equation in the form $\eta = \eta(\rho,T)$ in the low density region can be described through a Taylor series expansion in density around $\rho=0$, that is

$$\begin{aligned}\eta(\rho,T) &= \eta|_{\rho=0} + \left.\frac{\partial \eta}{\partial \rho}\right|_{\rho=0} \cdot \rho + \ldots \\ &= \eta^{(0)}(T) + \eta^{(1)}(T)\rho + \ldots. \\ &= \eta^{(0)}(T)\cdot[1 + B_\eta(T)\rho + \ldots], \end{aligned} \tag{8}$$

where $\eta^{(0)}$, $\eta^{(1)}$, and B_η are usually known in the literature as zero-density limit, initial density dependence, and second viscosity virial coefficient, respectively. These functions depend on temperature only.

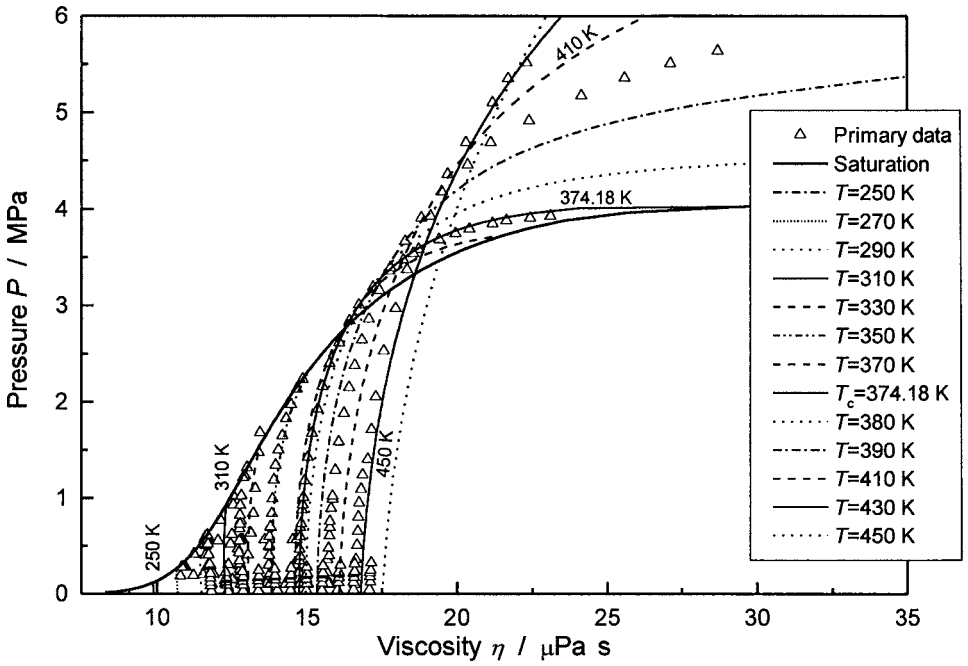

FIG. 10. Isotherms and saturation curve calculated from Eq. (4) on a P,η plane for the vapor phase close to the critical point.

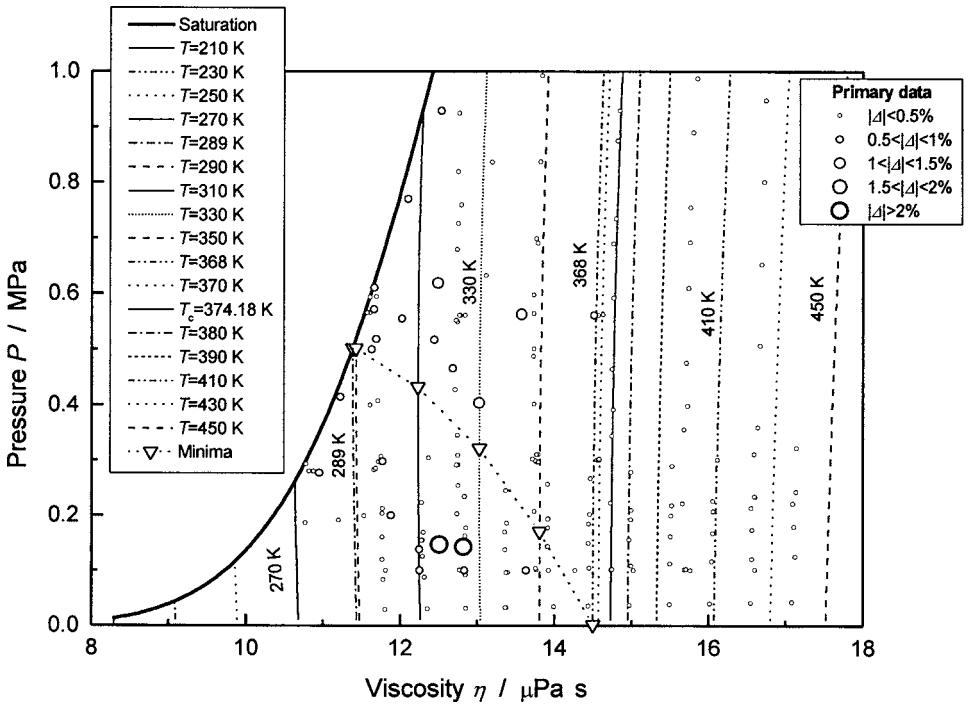

FIG. 11. Isotherms and saturated-vapor line calculated from Eq. (4), plotted on a P,η plane. Viscosity minima are found along a line in the low-density gas region.

Expanding Eq. (4) according to the truncated series of Eq. (8), the following two equations are obtained:

$$\eta^{(0)}(T)=H_c(e^{n_3T_r+n_5T_r^2}-1) \tag{9}$$

$$\eta^{(1)}(T)=\frac{H_c}{\rho_c}(n_8+n_9T_r^2)\cdot e^{n_3T_r+n_5T_r^2} \tag{10}$$

TABLE 9. Location of the viscosity minima in the dilute-gas region

T (K)	$P_{\min}$ (MPa)	$\eta_{\min}$ (μPa s)
289	0.501	11.381
310	0.432	12.228
330	0.321	13.024
350	0.170	13.807
368	0	14.497

TABLE 10. Deviations between accurate experimental data and values calculated from the new viscosity equation, Eq. (4), in the vapor region close to the reported viscosity minima

Reference	First author	Phase	NPT	T range (K)	P range (MPa)	AAD (%)	Bias (%)	MAD (%)
				$P<1.0$ MPa				
38	Assael	v	19	274–333	0.14–0.93	0.72	−0.23	2.59
39	Dowdell	v	6	308–403	0.1	0.48	0.13	0.65
42	Pasekov	v	37	275–371	0.28–0.60	0.30	−0.05	1.39
44	Shibasaki	v	61	298–423	0.1–1.00	0.19	0.02	0.77
45	Wilhelm	v	71	297–438	0.03–0.32	0.08	0.04	0.33
38	Assael	sv	4	273–303	0.29–0.77	0.71	0.71	1.00
	Overall		198			0.24	0.01	—
				$P<0.5$ MPa				
38	Assael	v	12	274–333	0.14–0.50	0.84	−0.59	2.59
39	Dowdell	v	6	308–403	0.1	0.48	0.13	0.65
42	Pasekov	v	24	275–371	0.28–0.31	0.25	0.05	0.90
44	Shibasaki	v	34	298–423	0.1–0.50	0.18	0.08	0.44
45	Wilhelm	v	71	297–438	0.03–0.32	0.08	0.04	0.33
38	Assael	sv	2	273–283	0.29–0.41	0.45	0.45	0.65
	Overall		149			0.21	0.01	—

TABLE 11. Variables and parameters of Eq. (7) for the locus of the viscosity minima found along isotherms in the low-density gas region

x	y	a	b	c
T_r	P_r	−0.747695	2.475032	−1.743515
T_r	ρ_r	0.124757	0.001619394	−0.130632
T_r	η_r	−0.0288930	0.624494	−0.134935

The values of the coefficients and parameters used in Eqs. (9) and (10), which are identical to those used in Eq. (4), are reported in Table 13.

However, Eq. (9) represents the extrapolation of the viscosity surface at the physical condition of zero pressure, even if it cannot be experimentally verified exactly at this condi-

TABLE 12. Statistical analysis of the representation of the primary data set by Eq. (4) and by the conventional equations of Krauss *et al.*[11] and Huber *et al.*[50] Only data within the validity limits of the Krauss equation were considered

				Eq. (4)			Krauss *et al.*[11] equation			Huber *et al.*[50] equation			
Reference	First author	Phase	NPT	ADD (%)	Bias (%)	MAD (%)	ADD (%)	Bias (%)	MAD (%)	ADD (%)	Bias (%)	MAD (%)	Class Eq. (4)
						Liquid							
26	Okubo	*l*	31	1.03	−0.92	2.12	1.57	−1.56	3.30	0.47	−0.02	1.31	I
27	Oliveira	*l*	43	1.18	1.01	2.91	0.96	0.88	3.44	2.19	2.19	3.61	I
29	Ruvinskij	*l*	16	1.29	−1.29	2.66	0.78	−0.78	1.64	0.39	−0.01	1.03	I
31	Heide	*sl*	7	1.57	−1.57	3.05	0.73	−0.55	2.20	0.73	−0.10	1.56	I
33	Laesecke	*sl*	52	0.77	0.00	1.96	1.12	0.93	2.81	1.47	1.43	3.00	I
27	Oliveira	*sl*	6	0.94	0.94	2.08	1.82	1.82	3.43	2.36	2.36	3.53	I
	Primary		155	1.03	−0.07	—	1.14	0.21	—	1.36	1.17	—	
24	Assael	*l*	24	2.21	2.21	2.77	1.83	1.83	2.63	3.20	3.20	3.57	II
25	Diller	*l*	20	7.80	7.80	10.15	7.28	7.28	10.68	8.67	8.67	11.39	II
28	Padua	*l*	11	2.89	2.55	3.73	2.56	2.56	3.88	3.68	3.68	4.71	II
24	Assael	*sl*	5	1.99	1.99	2.09	2.76	2.76	2.98	3.38	3.38	3.46	II
25	Diller	*sl*	7	7.42	7.42	8.56	8.06	8.06	9.27	8.72	8.72	9.89	II
30	Han	*sl*	9	2.82	2.82	6.41	3.56	3.56	7.29	4.20	4.20	7.77	II
32	Kumagai	*sl*	6	5.12	5.12	10.66	5.95	5.95	11.89	6.47	6.47	11.98	II
34	Padua	*sl*	1	3.55	3.55	3.55	4.18	4.18	4.18	4.89	4.89	4.89	II
35	Ripple	*sl*	5	3.60	3.60	5.93	4.26	4.26	6.57	4.94	4.94	7.22	II
36	Sagaidakova	*sl*	9	3.73	−3.73	4.53	2.66	−2.66	3.70	2.16	−2.16	3.01	II
37	Shankland	*sl*	7	12.60	12.60	23.51	13.33	13.33	24.57	13.84	13.84	24.64	II
	Total		259	2.56	1.62	—	2.61	1.86	—	3.10	2.83	—	
						Vapor							
38	Assael	*v*	20	0.71	−0.28	2.59	2.78	−2.78	4.30	0.83	−0.21	2.77	I
39	Dowdell	*v*	6	0.48	0.13	0.65	1.27	−1.27	1.67	0.40	−0.01	0.51	I
42	Pasekov	*v*	33	0.29	−0.09	1.39	2.16	−2.16	3.41	0.42	−0.11	1.56	I
44	Shibasaki	*v*	113	0.19	0.00	0.77	1.49	−1.34	4.12	0.22	−0.04	1.18	I
45	Wilhelm	*v*	65	0.08	0.04	0.33	1.35	−1.35	1.94	0.11	−0.11	0.26	I
38	Assael	*sv*	5	0.92	0.14	1.84	3.31	−3.31	5.47	1.23	0.73	1.60	I
	Primary		242	0.24	−0.02	—	1.68	−1.61	—	0.29	−0.07	—	
40	Mayinger	*v*	194	3.65	3.65	11.08	2.44	2.32	10.49	3.52	3.52	11.47	II
41	Nabizadeh	*v*	35	3.80	3.80	12.64	2.95	2.23	11.30	3.86	3.86	13.20	II
29	Ruvinskij	*v*	6	1.55	−1.28	3.04	2.26	−2.00	4.34	1.78	−1.50	3.39	II
43	Schramm	*v*	5	1.39	1.39	2.58	0.91	−0.04	1.84	1.19	1.19	2.47	II
40	Mayinger	*sv*	14	4.89	4.89	10.62	2.44	1.71	8.09	5.47	5.47	11.22	II
46	Oliveira	*sv*	6	2.69	2.69	3.63	0.87	−0.66	2.72	3.27	3.27	4.19	II
	Total		502	1.99	1.83	—	2.07	0.29	—	2.00	1.78	—	
						Supercritical							
26	Okubo	*sc*	8	0.93	0.39	1.27	0.77	−0.74	2.45	0.74	−0.28	2.22	I
44	Shibasaki	*sc*	13	0.24	−0.06	0.59	0.79	0.58	1.76	0.28	−0.14	0.76	I
	Primary		21	0.51	0.11	—	0.79	0.08	—	0.46	−0.19	—	
40	Mayinger	*sc*	17	12.21	12.21	15.14	12.59	12.59	14.86	11.96	11.96	15.19	II
41	Nabizadeh	*sc*	6	11.14	11.14	12.96	12.12	12.12	13.28	10.65	10.65	12.03	II
29	Ruvinskij	*sc*	5	1.59	1.59	2.30	1.80	1.80	2.96	2.07	2.07	3.63	II
	Total		49	5.98	5.81	—	6.37	6.07	—	5.86	5.58	—	
						Overall							
Overall primary			418	0.55	−0.03	—	1.44	−0.85	—	0.70	0.38	—	
Overall			810	2.41	2.01	—	2.50	1.14	—	2.58	2.35	—	

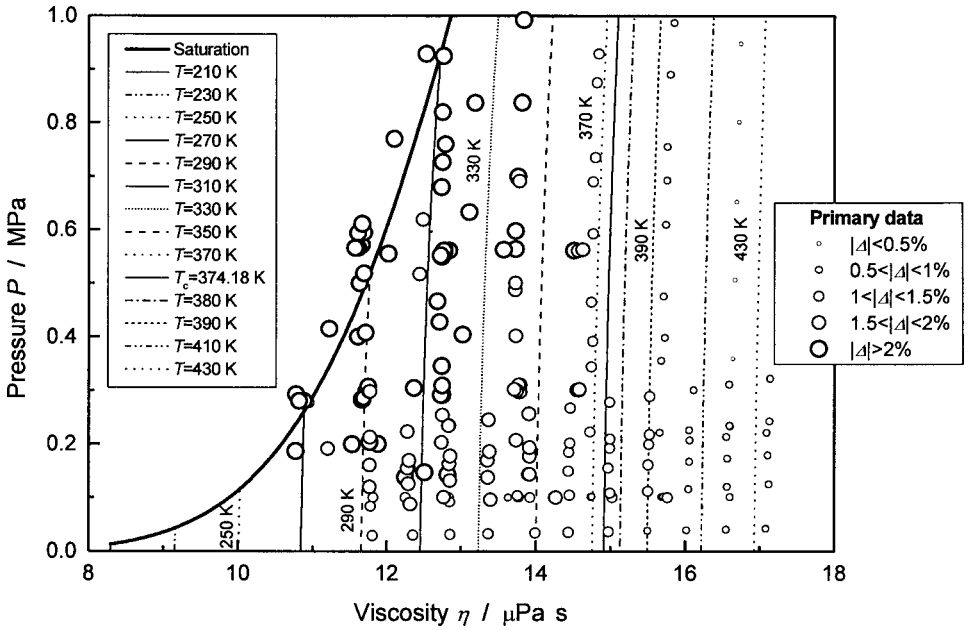

FIG. 12. Isotherms and saturated-vapor line calculated from the equation by Krauss *et al.*,[11] plotted on a P,η plane.

tion. Therefore, when the mean free path of the gas is comparable to the dimensions of the confining medium the viscosity equation is intended not to be valid.[52]

7.1. Calculation of the Scaling Factors

The calculation of the fluid specific scaling factors ε/k and σ is necessary to compare the new viscosity equation with experimental data and with models from the literature, which are usually presented in a unified reduced format. The energy and the length scaling parameters, respectively, are used in the literature to obtain dimensionless models and to transfer models to different target fluids. The values of the corresponding parameters have to be regressed from viscosity experimental data in the dilute-gas region. In this work it was necessary to update the values for R134a, published by Krauss *et al.*,[11] in order to consider the more recent data as well. The procedure used is described further on.

An equation for the dilute-gas region was developed to obtain the scaling factors characterizing this range of states. Only the experimental data already selected as primary and with $\rho<0.15$ mol L^{-1}, i.e., $\rho<15.3$ kg m^{-3}, have been considered for the study of the dilute-gas region.

The deviations between these data and values calculated from the multiparameter viscosity equation, Eq. (4), and from the conventional equations by Krauss *et al.*[11] and Huber *et al.*[50] are reported in Table 14.

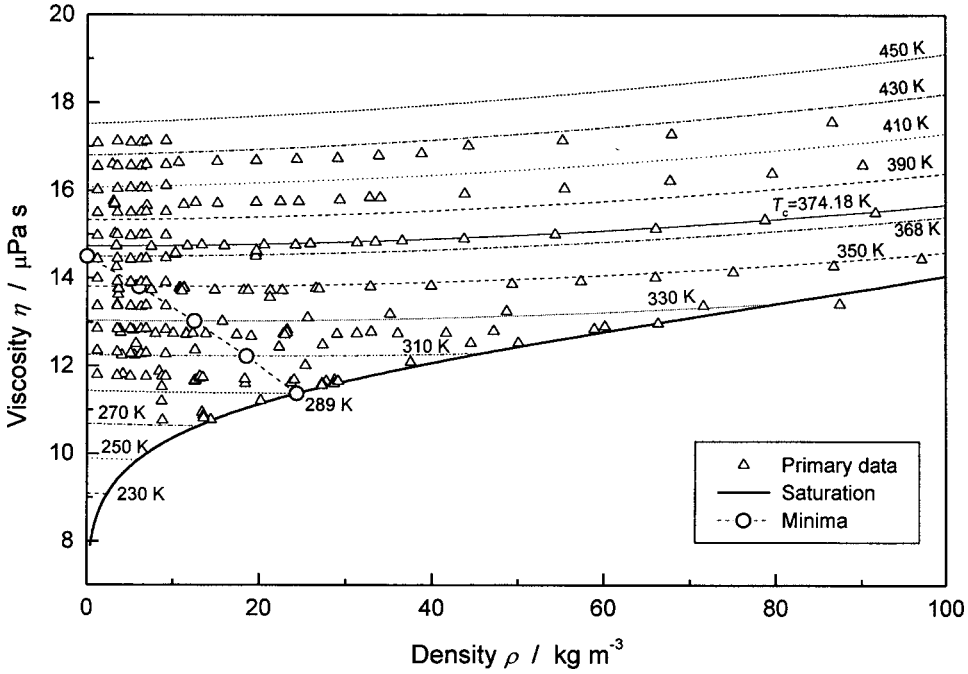

FIG. 13. Experimental data and viscosity values calculated from Eq. (4) along isotherms and the saturation line in the vapor region.

TABLE 13. Coefficients and parameters used in Eqs. (9) and (10)

T_c (K)	374.18
ρ_c (kg m^{-3})	508.0
H_c (μPa s)	25.17975
n_3	0.5668165
n_5	−0.1061795
n_8	−0.1621088
n_9	0.1675102

Based on these data, a regression with the optimization algorithm gave the following equation, with the variables defined as in Eq. (12) and the parameters and coefficients reported in Table 15:

$$\eta_{r,\mathrm{ld}} = \sum_{i=1}^{6} n_i T_r^{g_i} \rho_r^{h_i} \tag{11}$$

where

$$\eta_{r,\mathrm{ld}} = \frac{\eta}{H_c}$$

$$T_r = \frac{T}{T_c} \tag{12}$$

$$\rho_r = \frac{\rho}{\rho_c}.$$

A statistical analysis of the deviations between values calculated from Eq. (11) and the selected data is reported in Table 16. A comparison with Table 14 shows that Eq. (11) results in a lower AAD and a bias closer to zero than Eq. (4) in this region.

At the zero-density limit, the Taylor series expansion of Eq. (11), as shown by Eq. (8), results in the following equations, for which the parameters and coefficients are given in Table 15:

$$\eta_{\mathrm{zd}}^{(0)}(T) = H_c(n_1 T_r + n_2 T_r^{3.5}) \tag{13}$$

$$\eta_{\mathrm{zd}}^{(1)}(T) = \frac{H_c}{\rho_c}(n_3 T_r^4 + n_4 T_r^{4.5} + n_5 T_r^{5.5} + n_6 T_r^6) \tag{14}$$

TABLE 15. Parameters and coefficients of Eq. (11)

T_c (K)			374.18
ρ_c (kg m^{-3})			508.0
H_c (μPa s)			25.17975
i	g_i	h_i	n_i
1	1.0	0	0.5968838
2	3.5	0	−0.01190498
3	4.0	1	14.15581
4	4.5	1	−34.02928
5	5.5	1	43.56207
6	6.0	1	−23.65639

where the subscript zd indicates the condition at the zero-density limit.

Once these equations are obtained, the scaling factors ε/k and σ, which are necessary for the following developments, can be determined. In the conventional equation by Krauss *et al.* the dilute-gas term $\eta_{\mathrm{conv}}^{(0)}$ [Eq. (7) from Krauss *et al.*[11]], which was derived from the kinetic theory of gases, is given in a generalized form. The resulting formulation is usually adapted to a target fluid by fitting the scaling factors ε/k and σ to experimental data extrapolated to zero density. The basic idea of this section is to determine the values of these parameters in a way that the equation for $\eta_{\mathrm{conv}}^{(0)}$ matches as closely as possible Eq. (13), which was obtained from experimental data only.

For the collision integral $\Omega_\eta(T^*)$, which is included in the cited equation for $\eta_{\mathrm{conv}}^{(0)}$, the same functional form and coefficients a_i used by Krauss *et al.*[11] [Eqs. (10) and (11)] were assumed. The scaling factors ε/k and σ have consequently been determined by minimizing the function

$$\chi_{\mathrm{zd}}^2\left(\frac{\varepsilon}{k},\sigma\right) = \int_{T_1}^{T_2} \left[\frac{\eta_{\mathrm{zd}}^{(0)} - \eta_{\mathrm{conv}}^{(0)}\left(\frac{\varepsilon}{k},\sigma\right)}{\eta_{\mathrm{zd}}^{(0)}}\right]^2 \mathrm{d}T \tag{15}$$

where $T_1 = 273$ K and $T_2 = 437$ K are the temperature limits of the experimental data range. The values obtained in the fitting procedure are reported in Table 17. The statistical quantities reported in this table were determined with the following functions, where $\eta_{\mathrm{conv}}^{(0)}$ was calculated assuming the ε/k and σ values reported in Table 17, as well:

TABLE 14. Deviations between primary experimental data with $\rho < 15.3$ kg m^{-3} and values calculated from different viscosity equations

			Eq. (4)			Krauss *et al.*[11]			Huber *et al.*[50]		
Reference	First author	NPT	AAD (%)	Bias (%)	MAD (%)	AAD (%)	Bias (%)	MAD (%)	AAD (%)	Bias (%)	MAD (%)
39	Dowdell	6	0.48	0.13	0.65	1.27	−1.27	1.67	0.40	−0.01	0.51
42	Pasekov	24	0.25	0.05	0.90	1.91	−1.91	2.63	0.33	−0.01	1.06
44	Shibasaki	29	0.17	0.13	0.44	1.28	−1.28	2.39	0.15	−0.02	0.39
45	Wilhelm	71	0.08	0.04	0.33	1.29	−1.29	1.94	0.12	−0.12	0.37
Overall primary		130	0.15	0.06	—	1.40	−1.40	—	0.18	−0.07	—

TABLE 16. Deviations between the selected data and values calculated from Eq. (11)

			Eq. (11)		
Reference	First author	NPT	AAD (%)	Bias (%)	MAD (%)
39	Dowdell	6	0.40	0.05	0.58
42	Pasekov	24	0.19	−0.04	0.60
44	Shibasaki	29	0.16	0.09	0.46
45	Wilhelm	71	0.05	−0.03	0.15
Overall		130	0.12	0.00	—

$$r_{zd}^2 = 1 - \frac{\int_{T_1}^{T_2} (\eta_{zd}^{(0)} - \eta_{conv}^{(0)})^2 dT}{\int_{T_1}^{T_2} (\eta_{zd}^{(0)} - \eta_{zd}^{mean})^2 dT} \quad (16)$$

$$\eta_{zd}^{mean} = \frac{\int_{T_1}^{T_2} \eta_{zd}^{(0)}\, dT}{T_2 - T_1} \quad (17)$$

$$AAD_{zd}\% = \frac{100}{T_2 - T_1} \int_{T_1}^{T_2} \left| \frac{\eta_{zd}^{(0)} - \eta_{conv}^{(0)}}{\eta_{zd}^{(0)}} \right| dT \quad (18)$$

$$Bias_{zd}\% = \frac{100}{T_2 - T_1} \int_{T_1}^{T_2} \frac{\eta_{zd}^{(0)} - \eta_{conv}^{(0)}}{\eta_{zd}^{(0)}} dT \quad (19)$$

$$MAD_{zd}\% = \underset{[T_1, T_2]}{\text{Max}} \left(100 \left| \frac{\eta_{zd}^{(0)} - \eta_{conv}^{(0)}}{\eta_{zd}^{(0)}} \right| \right). \quad (20)$$

The values obtained for the scaling factors have been used to process the experimental data and to compare them with the results derived from Eq. (4) and from Eq. (11).

The reduced second viscosity virial coefficient B_η^* and the reduced temperature T^* can be now calculated according to Vogel *et al.*[53]

$$B_\eta^* = \frac{M}{N_A \sigma^3} \cdot \frac{\eta^{(1)}}{\eta^{(0)}} \quad (21)$$

$$T^* = \frac{kT}{\varepsilon} \quad (22)$$

where M is the molar mass and N_A is the Avogadro number.

TABLE 17. Results of the fitting procedure

ε/k (K)	σ (nm)	r_{zd}^2	AAD_{zd} (%)	$Bias_{zd}$ (%)	MAD_{zd} (%)
284.517	0.508692	0.999887	0.1182	2.17×10^{-4}	0.3693

TABLE 18. Results from data by Shibasaki *et al.*[44]

T (K)	$\eta^{(0)}$ (μPa s)	$\eta^{(1)}$ (μPa s m^3 kg^{-1})	T^*	B_η^*	NPT	r^2
298.150	11.840748	−0.007201	1.0479	−0.782626	3	0.950
323.150	12.768388	−0.001997	1.1358	−0.201314	5	0.460
348.150	13.770947	−0.003093	1.2237	−0.289095	6	0.502
373.150	14.731304	0.001465	1.3115	0.128020	5	0.247
398.150	15.679142	0.001897	1.3994	0.155701	6	0.151
423.150	16.574071	0.006125	1.4873	0.475584	4	0.934

7.2. Calculation of Quasiexperimental $\eta^{(0)}$ and B_η^* Values

To allow for a comparison of the experimental data with the models available for this region the data were converted into the format used in the models. Quasiexperimental values were generated in this way.

In the dilute-gas region there are four primary viscosity data sets, from which quasiexperimental $\eta^{(0)}$ and B_η^* values could be calculated. To account only for the points in the dilute-gas region, data at $\rho > 15.3$ kg m^{-3} were rejected. In the following paragraphs each of these data sets is examined in detail. The values of T^* and B_η^* are calculated by means of Eqs. (21) and (22) with the parameters reported in Table 17.

7.2.1. Data by Shibasaki *et al.*[44]

The data set by Shibasaki *et al.*[44] presents viscosity values measured along isotherms. Six isothermal groups were set up and each of them was fitted using a linear equation of the form:

$$\eta = \eta^{(0)} + \eta^{(1)} \cdot \rho. \quad (23)$$

In Table 18 the results of these fits are reported together with the number of data points along each isotherm and the correlation coefficient, r^2, which is defined as

$$r^2 = 1 - \frac{\sum_{i=1}^{NPT} (\eta_{exp} - \eta_{calc})_i^2}{\sum_{i=1}^{NPT} (\eta_{exp} - \eta_{exp}^{mean})_i^2} \quad (24)$$

$$\eta_{exp}^{mean} = \frac{\sum_{i=1}^{NPT} (\eta_{exp})_i}{NPT}. \quad (25)$$

TABLE 19. Parameters and coefficients for Eq. (26)

T_c (K)	374.18
ρ_c (kg m^{-3})	508.0
H_c (μPa)	25.17975

i	g_i	h_i	n_i
1	0.5	1	−6.383642
2	1.0	0	0.6254408
3	1.0	1	11.79207
4	1.5	0	-3.831399×10^{-2}
5	1.5	1	−5.356507
6	4.0	0	-2.568288×10^{-3}

TABLE 20. Statistical analysis of deviations between values calculated from Eq. (26) and the data by Wilhelm and Vogel[45]

NPT	71
AAD%	0.03
Bias%	0.00
MAD %	0.12

The low values of r^2 for most of the isotherms show that in these cases the data correlation is not of a good quality.

7.2.2. Data by Wilhelm and Vogel[45]

The data by Wilhelm and Vogel[45] are presented in isochoric groups. Nevertheless, they can be divided into 11 quasi-isothermal groups, each of them covering a temperature range that can be contained in a span of 2 K. Equation (26), with the variables defined in Eq. (12) and the coefficients presented in Table 19, was obtained by fitting these data

$$\eta_{r,ld} = \sum_{i=1}^{6} n_i T_r^{g_i} \rho_r^{h_i}. \tag{26}$$

Deviations between values calculated from this equation and the data are reported in Table 20. Equation (26) results in an excellent representation of the data themselves.

The following equations for the zero-density limit and for the initial density dependence result from expanding Eq. (26) in a Taylor series. Values of the parameters and coefficients are reported in Table 19:

$$\eta^{(0)}_{\text{Wilhelm}}(T) = H_c(n_2 T_r + n_4 T_r^{1.5} + n_6 T_r^4), \tag{27}$$

$$\eta^{(1)}_{\text{Wilhelm}}(T) = \frac{H_c}{\rho_c}(n_1 T_r^{0.5} + n_3 T_r + n_5 T_r^{1.5}). \tag{28}$$

With Eqs. (27), (28), (21), and (22), the values of the quantities $\eta^{(0)}$, $\eta^{(1)}$, B^*_η, and T^* were calculated at the mean temperature of each of the quasi-isothermal groups in which the experimental data were divided. These values are reported in Table 21, together with the deviations resulting from Eq. (26) with respect to the data of each group.

7.2.3. Other Data Sets

The data sets of Dowdell *et al.*[39] and Pasekov *et al.*[42] cannot be used for comparisons in reduced form, because they contain only a limited number of data points not measured along isotherms. In fact it is neither possible to process them as it has been done for the Shibasaki *et al.* isothermal data, nor to follow the technique applied for the Wilhelm and Vogel data, because the number of data points is too small to develop a reliable individual correlation in the low-density region.

7.3. Comparison of Models and Experimental Data

The equations derived from the multiparameter viscosity Eq. (4), i.e., Eqs. (9), (10), and (21), are plotted in Figs. 14–16 together with the equations derived from the viscosity Eq. (11), i.e., Eqs. (13), (14), and (21). Comparisons with the $\eta^{(0)}_{\text{conv}}$ and $\eta^{(1)}_{\text{conv}}$ functions of the conventional equations,[11,50] with the B^*_η function from Vogel *et al.*,[53] and with experimental data are presented as well.

The work of Krauss *et al.*[11] did not develop the initial density dependence term for R134a, but they considered a single term including the initial density dependence term and the excess term. For sake of comparison, the corresponding function $\eta^{(1)}_{\text{conv}}(T)$ has been calculated expanding the viscosity equation from Krauss *et al.*[11] in a Taylor series in density around $\rho = 0$:

$$\eta_{\text{conv}}(T,\rho) = \eta_{\text{conv}}(T,\rho)\big|_{\rho=0} + \eta'_{\text{conv}}(T,\rho)\big|_{\rho=0} \cdot \rho + \ldots\ldots. \tag{29}$$

Keeping the same formalism of the cited equation in Krauss *et al.*[11] this approach results in Eq. (30), with the parameters listed in Table 22:

$$\eta^{(1)}_{\text{conv}}(T) = \eta'_{\text{conv}}(T,\rho)\big|_{\rho=0} = \frac{H_{c,\text{conv}}}{\rho_{c,\text{conv}}}\left(e_1 - \frac{e_4}{e_5^2}\right). \tag{30}$$

TABLE 21. Results from data by Wilhelm and Vogel[45]

T (K)	$\eta^{(0)}$ (μPa s)	$\eta^{(1)}$ (μPa s m^3 kg^{-1})	T^*	B^*_η	NPT	AAD (%)	Bias (%)	MAD (%)
297.478	11.809943	−0.005653	1.0456	−0.615994	5	0.023	−0.020	0.052
310.890	12.322650	−0.003863	1.0927	−0.403421	7	0.021	0.003	0.049
324.760	12.851069	−0.002166	1.1414	−0.216882	7	0.053	0.053	0.075
338.636	13.377854	−0.000627	1.1902	−0.060335	8	0.043	−0.022	0.119
353.064	13.923529	0.000801	1.2409	0.074057	8	0.042	−0.023	0.061
366.752	14.439259	0.001993	1.2890	0.177665	6	0.016	−0.007	0.036
380.808	14.966826	0.003051	1.3384	0.262349	6	0.018	−0.001	0.045
394.735	15.487397	0.003932	1.3874	0.326694	6	0.033	0.011	0.050
409.290	16.029131	0.004673	1.4385	0.375167	6	0.028	0.017	0.043
423.100	16.540872	0.005207	1.4871	0.405088	6	0.022	0.002	0.041
437.840	17.084558	0.005594	1.5389	0.421360	6	0.033	−0.010	0.069

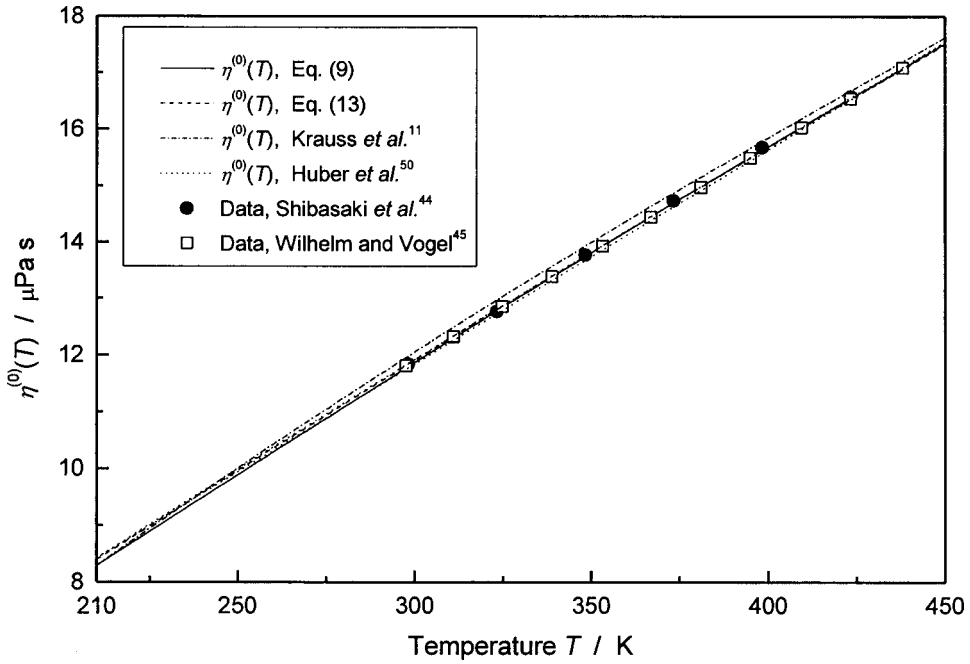

FIG. 14. Results for the zero-density limit $\eta^{(0)}(T)$, calculated from Eq. (9) derived from Eq. (4), from Eq. (13) derived from Eq. (11), from the conventional equations $\eta^{(0)}_{\text{conv}}$ from Krauss *et al.*[11] and Huber *et al.*,[50] and from the available experimental data.

It is evident that Eq. (30) does not depend on temperature, in fact it results in a constant value of $\eta^{(1)}_{\text{conv}} = 2.51655 \times 10^{-3}$ μPa s m^3 kg^{-1}.

Figure 14 compares the viscosity zero-density limits $\eta^{(0)}(T)$ calculated from Eqs. (9) and (13) from the conventional equations $\eta^{(0)}_{\text{conv}}$ from Krauss *et al.*,[11] and Huber *et al.*,[50] and from the available reduced experimental data.[44,45]

In Fig. 15 the viscosity initial density dependencies $\eta^{(1)}(T)$ calculated from Eqs. (10), (14), and (30) from the conventional equation of Krauss *et al.*,[11] and from the conventional equation of Huber *et al.*,[50] are compared with the available reduced experimental data.[44,45]

Figure 16 shows the plot of the $B^*_\eta(T^*)$ equation by Vogel *et al.*,[53] which is an enhancement of the Rainwater–Friend theory[54,55] and is recommended for propane and as a general approach for the other fluids. The same equation was also used by Huber *et al.*[50] In the same figure the $B^*_\eta(T^*)$ functions for the present viscosity equation, Eq. (21) from Eqs. (9) and (10), and for the low-density equation, Eq. (21) from Eqs. (13) and (14), are plotted together with the available reduced experimental data.[44,45]

For the zero-density limit, Fig. 14 shows very good agreement among Eq. (9), the low density Eq. (13), the conventional equation from Huber *et al.*,[50] and both experimental

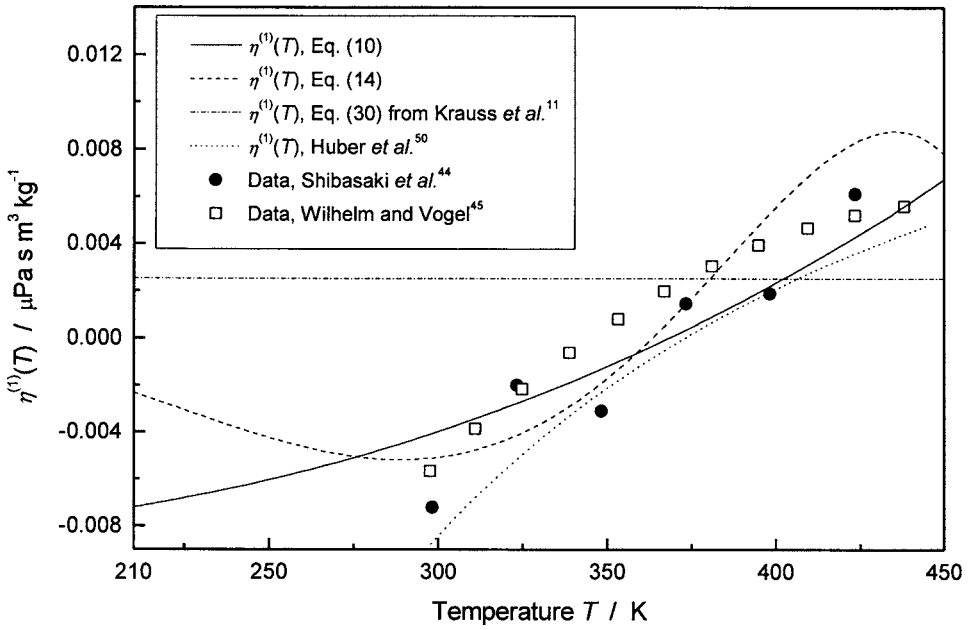

FIG. 15. Results for the viscosity initial density-dependence $\eta^{(1)}(T)$, calculated from Eq. (10) derived from Eq. (4), from Eq. (14) derived from Eq. (11), from Eq. (30) derived from the conventional equation,[11] from the conventional equation,[50] and from the available experimental data.

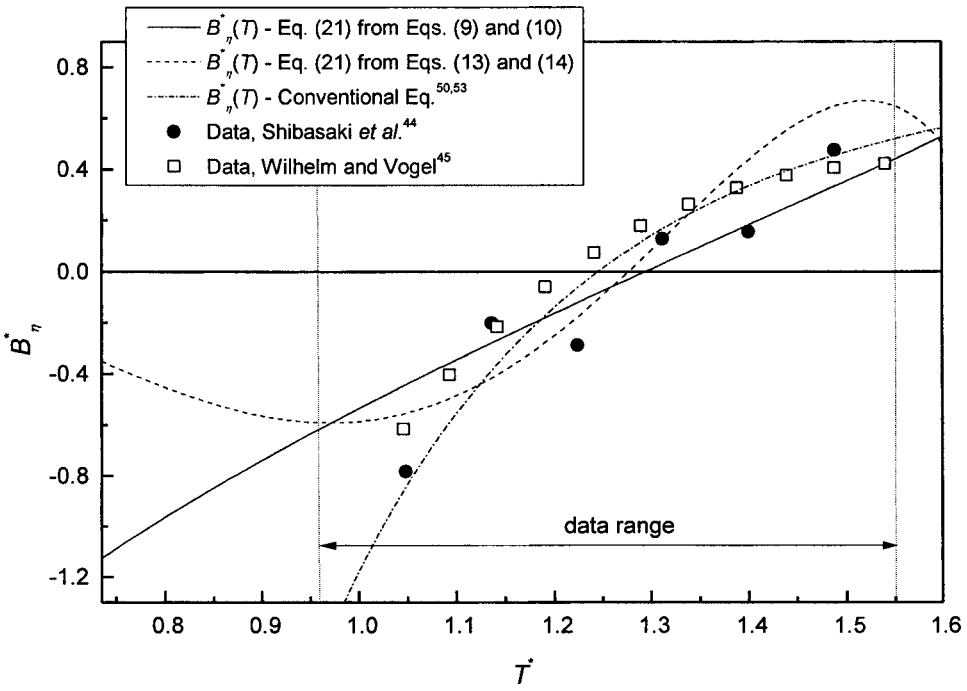

FIG. 16. Results for the reduced second viscosity virial coefficient B^*_η as a function of reduced temperature T^* calculated for Eq. (21), which was derived from Eqs. (9) and (10), for the low density equation, Eq. (21), which was derived from Eqs. (13) and (14), for the conventional equation,[50,53] and for the available experimental data.

data sets. The conventional equation from Krauss *et al.*[11] is slightly less accurate with respect to the data.

For the initial density dependence, Fig. 15 reflects a lower precision, because all four equations, Eq. (10), the low-density Eq. (14), the equation from Huber *et al.*,[50] and Eq. (30) from Krauss *et al.*,[11] do not correctly represent the data. Results calculated from Eq. (10) basically follow the data trend. The low-density Eq. (14) is far less accurate and Eq. (30), derived from Krauss *et al.*,[11] does not represent the trend of the data at all.

For the reduced second viscosity virial coefficient B^*_η, as shown in Fig. 16, the conventional equation from Huber *et al.*[50] and Vogel *et al.*[53] represents the data slightly better than the equations presented here, but the equation derived from Eq. (4) reaches a comparable level of accuracy in the data range. The low-density equation yields an unreasonable plot, even though this equation represents the experimental data in the region with very high accuracy (see Table 16).

The three equations available for B^*_η cross the zero line in a range of reduced temperature T^* of 1.25–1.30. This corresponds to a temperature range from 355.6 to 369.9 K. The data from the two evaluated references confirm this trend. The B^*_η function derived from Eq. (4) crosses the zero line at $T=368$ K. If B^*_η becomes zero this corresponds to a value of zero for $\eta^{(1)}(T)$ and the corresponding isothermal line intercepts the $\rho=0$ limit with a horizontal slope on a $\eta-\rho$ plane. Looking at Fig. 13, which shows the locus of the isothermal minima calculated from Eq. (4), this behavior is verified for a temperature of about 368 K. The same value can be read from Fig. 11 for the isotherm presenting a viscosity minimum at $P=0$.

Notwithstanding the Wilhelm and Vogel[45] data are very accurately represented by Eq. (4), the Fig. 16 shows that the corresponding Eq. (21) presents appreciable error deviations with respect to the same data set. The correct representation of a viscosity equation in the dilute-gas region by the form $B^*_\eta(T^*)$ requires in fact an extremely high accuracy level of the equation itself and it does not bring a real benefit for the viscosity surface representation. As a consequence for the present fluid the traditional initial density dependence analysis does not match the high accuracy reached by the present heuristic method.

TABLE 22. Parameters of Eq. (30)

$H_{c,\mathrm{conv}}$ (μPa s)	25.21
$\rho_{c,\mathrm{conv}}$ (kg m^{-3})	515.25
e_1	−1.89758
e_4	−23.1648
e_5	3.44752

8. Planning of the Data Points Needed for Developing a Viscosity Equation

Considering the interesting results achieved in this work, a question can be posed about the number of primary data needed for the equation development with the proposed technique and the required arrangement of the points on the surface. In general for a heuristic method difficulties are brought in by the nonhomogeneous distribution of the experimental data and by their error noise.

TABLE 23. Variation of the prediction accuracy of a multiparameter viscosity equation with the reduction of the number of points of the regression set

Data used for regression				Comparison with all the data			
NPT	AAD (%)	Bias (%)	MAD (%)	NPT	AAD (%)	Bias (%)	MAD (%)
1024	0.02	0.00	0.34	4096	0.02	0.00	0.61
512	0.02	0.00	0.25	4096	0.02	0.00	0.53
256	0.02	0.00	0.13	4096	0.02	0.00	0.27
128	0.02	0.00	0.20	4096	0.02	0.00	0.63
64	0.02	0.00	0.11	4096	0.02	0.00	0.37
32	0.01	0.00	0.06	4096	0.04	0.00	0.42
16	0.01	0.00	0.05	4096	0.09	−0.01	0.47

To analyze the posed problem it is convenient to use data generated by a viscosity equation, which is a reliable representation of the screened experimental data. The conventional equation by Krauss *et al.*[11] was used here for the study.

A regular grid was at first defined: the temperature validity range for the equation is 290–430 K and was divided into 63 equal intervals of 2.2 K. The pressure range from 0.05 to 9.5 MPa was similarly divided into 63 equal intervals of 0.15 MPa. The P,T grid thus contains 4096 points.

The density was calculated at each point by the DEoS in the MBWR32 format, from Huber and McLinden[51] in order to enter the independent variables (T,ρ) into the viscosity equation to get the corresponding viscosity value. This DEoS is the same used by Krauss *et al.*[11] for the viscosity equation.

A regular grid of 4096 T,P,ρ,η points was then obtained. Regular grids of 1024, 512, 256, 128, 64, 32, and 16 points were extracted from the original grid, corresponding to 1/4, 1/8, 1/16, 1/32, 1/64, 1/128, and 1/256 of the original points.

From the former bank of terms, Eq. (2), and following the same regression technique previously presented, a viscosity equation was obtained from the points of each grid. Each equation was then validated with respect to the original grid of 4096 points. The reduction of the points of the regression set led to the results represented in Table 23 and Fig. 17.

From Table 23 one sees that the regression accuracy is always very high even with an extremely reduced number of points. On the other hand the validation accuracy on the whole data base tends to decrease only when the equation is regressed over less than about 60 points. Up to such a limit the proposed heuristic method always behaves very satisfactorily.

It is then evident that, through the proposed technique, a reduced number of experimental points is sufficient to successfully perform the regression of a dedicated viscosity equation. A number of points ranging from 50 to 100 and regularly distributed on the η,T,P surface seem to be sufficient, but only with the condition of good experimental accuracy. In fact the points used in this test are totally free from error noise.

This conclusion is of great importance in view of the economy of the experimental effort needed for the development of a dedicated viscosity equation.

9. Tabulations of the Viscosity Equation

Viscosity values of R134a generated from Eq. (4) for both the saturation line and the single phase regions are reported in Tables A1 and A2 of the Appendix. The density values and the saturation properties are obtained from the fundamental DEoS by Tillner-Roth and Baehr.[21] These tables can also be used as reference values for the validation of a computer code.

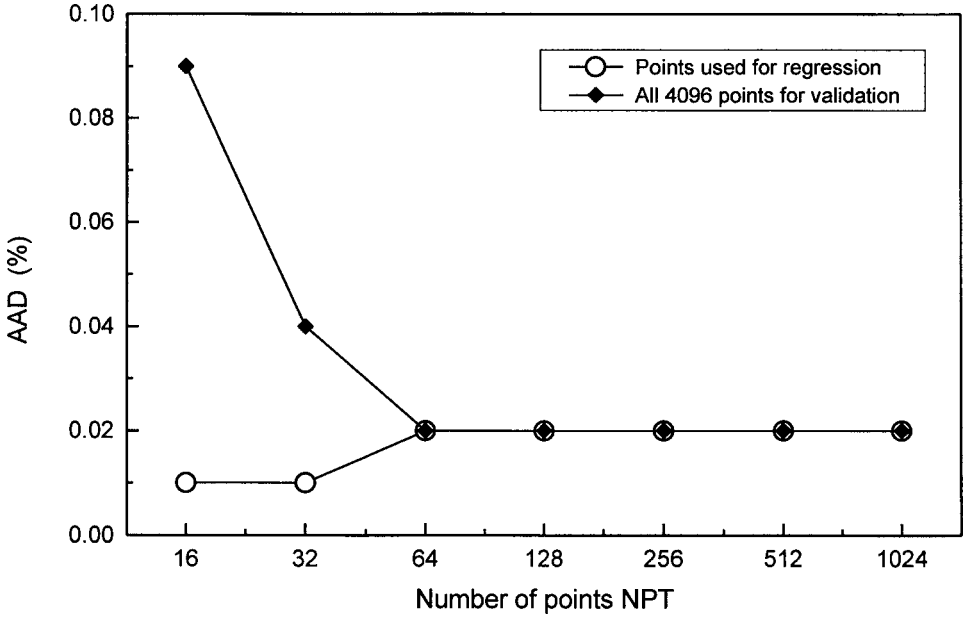

FIG. 17. Error deviation trends with varying number of regression points.

10. Conclusions

A new, completely correlative method directly based on the available viscosity data has been proposed for the development of viscosity equations. The new technique is based on the optimization algorithm of the functional form of multiparameter equations of state, set up by Setzmann and Wagner,[20] and has been applied for the development of a viscosity equation for the refrigerant R134a.

For the data sets considered reliable, the new multiparameter viscosity equation results in an AAD value of 0.55%, while for the same data base the equation by Krauss *et al.*[11] considered as a reference so far results in an AAD of 1.44%, while the equation by Huber *et al.*[50] yields an AAD of 0.70%. Furthermore, the new method can be used as a powerful tool for experimental data screening. The optimization procedure by Setzmann and Wagner is a promising tool for the development of viscosity equations. Equations developed using this tool are able to represent the whole viscosity surface well within the uncertainty of the experimental data. To fill the lack of data inside the validity range of the equation new experimental points are needed in the vapor region at low temperatures, in the liquid region at low pressures, and at high pressures and high temperatures, as it is evidenced by Fig. 1.

From the study of the new viscosity equation, two loci of minima on the viscosity surface have been found: one in the low density vapor region and the other in the dense-fluid region, mostly at supercritical conditions. Both lines of minima have been analytically represented.

The behavior of the new equation in the dilute-gas region has been compared with the theoretically founded Rainwater–Friend model for the second viscosity virial coefficient and with experimental data in the low-density vapor region. The virial expansion method used to study the viscosity surface in the low-density region demonstrates that it cannot contribute to improvement of the viscosity surface representation. In fact for the present fluid the initial density dependence analysis does not match the high accuracy reached by the present heuristic method.

A study has also been performed to find the minimum number of primary data needed for the equation development through the proposed technique. A limited number of experimental points, around 50 or so, is shown to be enough when supplied as input to the present correlative method in order to accurately represent the whole viscosity surface. The required conditions are a regular distribution of the points on the same surface and a good level of experimental uncertainty. This leads to an evident economy of the experimental effort needed for the development of a dedicated viscosity equation.

Nomenclature

a,b,c	adjustable parameters
AAD	average absolute deviation
B_η	second viscosity virial coefficient
B_η^*	reduced B_η
Bias	bias
e_1,e_4,e_5	equation parameters
g,h,n	adjustable parameters
H_c	pseudocritical viscosity
$\bar{n}$	vector of individual coefficients
M	molar mass
MAD	maximum average deviation
N	number of primary data
N_A	Avogadro number
NPT	number of data points
P	pressure
r	correlation coefficient
R	gas constant
T	thermodynamic temperature
T^*	reduced temperature
x	symbolic variable
y	symbolic variable

Greek

ε/k	energy scaling parameter
χ^2	sum of squares
Δ	error deviation
η	viscosity
$\eta^{(0)}$	viscosity in the zero-density limit
$\eta^{(1)}$	viscosity initial density dependence
ρ	mass density
σ	length scaling parameter
Ω_η	collision integral

Superscripts

mean	mean

Subscripts

c	at the critical point
calc	calculated
conv	conventional equation
exp	experimental
i,j	indices
ld	low density
min	at the minimum point
r	reduced
zd	at zero density limit

11. Appendix: Tables of Viscosity Values for R134a

TABLE A1. Viscosity of R134a along the saturation line

		Saturated liquid		Saturated vapor	
Temperature (K)	Pressure (MPa)	Density (kg m^{-3})	Viscosity (μPa s)	Density (kg m^{-3})	Viscosity (μPa s)
210.0	0.012910	1483.06	701.34	0.76222	8.2868
212.5	0.015245	1476.14	668.07	0.89064	8.3860
215.0	0.017919	1469.19	637.26	1.0361	8.4852
217.5	0.020969	1462.21	608.68	1.2003	8.5842
220.0	0.024433	1455.19	582.09	1.3850	8.6830
222.5	0.028352	1448.15	557.30	1.5919	8.7818
225.0	0.032769	1441.06	534.14	1.8231	8.8804
227.5	0.037732	1433.94	512.45	2.0804	8.9788
230.0	0.043287	1426.78	492.11	2.3660	9.0771
232.5	0.049486	1419.58	472.99	2.6820	9.1752
235.0	0.056380	1412.34	454.98	3.0309	9.2731
237.5	0.064026	1405.05	437.99	3.4150	9.3709
240.0	0.072481	1397.71	421.94	3.8367	9.4686
242.5	0.081804	1390.33	406.74	4.2988	9.5660
245.0	0.092057	1382.89	392.33	4.8039	9.6634
247.5	0.10330	1375.40	378.65	5.3548	9.7605
250.0	0.11561	1367.86	365.64	5.9546	9.8576
252.5	0.12905	1360.25	353.25	6.6062	9.9545
255.0	0.14368	1352.59	341.44	7.3129	10.051
257.5	0.15959	1344.85	330.16	8.0781	10.148
260.0	0.17684	1337.05	319.38	8.9052	10.245
262.5	0.19551	1329.18	309.05	9.7978	10.342
265.0	0.21567	1321.24	299.16	10.760	10.438
267.5	0.23742	1313.22	289.66	11.795	10.535
270.0	0.26082	1305.11	280.55	12.908	10.632
272.5	0.28597	1296.92	271.78	14.103	10.729
273.0	0.29122	1295.27	270.06	14.353	10.749
275.0	0.31294	1288.64	263.34	15.385	10.827
277.5	0.34182	1280.26	255.21	16.758	10.924
280.0	0.37271	1271.79	247.36	18.228	11.023
282.5	0.40568	1263.21	239.79	19.800	11.121
285.0	0.44083	1254.51	232.48	21.479	11.221
287.5	0.47826	1245.71	225.40	23.273	11.321
290.0	0.51805	1236.77	218.55	25.187	11.422
292.5	0.56031	1227.71	211.91	27.228	11.525
295.0	0.60512	1218.51	205.48	29.404	11.629
297.5	0.65259	1209.17	199.23	31.723	11.734
298.0	0.66241	1207.28	198.00	32.204	11.756
300.0	0.70282	1199.67	193.16	34.193	11.842
302.5	0.75591	1190.00	187.26	36.824	11.951
305.0	0.81197	1180.16	181.52	39.625	12.063
307.5	0.87109	1170.14	175.93	42.609	12.178
310.0	0.93340	1159.92	170.49	45.786	12.296
312.5	0.99899	1149.49	165.17	49.170	12.418
315.0	1.0680	1138.83	159.99	52.775	12.545
317.5	1.1405	1127.93	154.92	56.617	12.676
320.0	1.2166	1116.77	149.96	60.715	12.813
322.5	1.2965	1105.33	145.11	65.087	12.957
325.0	1.3803	1093.59	140.35	69.757	13.108
327.5	1.4680	1081.51	135.69	74.749	13.268
330.0	1.5599	1069.08	131.11	80.094	13.438
332.5	1.6561	1056.26	126.60	85.822	13.619
335.0	1.7566	1043.02	122.17	91.974	13.813
337.5	1.8617	1029.29	117.80	98.594	14.022
340.0	1.9715	1015.05	113.48	105.73	14.249
342.5	2.0862	1000.21	109.21	113.46	14.496
345.0	2.2059	984.71	104.97	121.84	14.767
347.5	2.3308	968.45	100.76	130.98	15.068
350.0	2.4611	951.32	96.564	140.99	15.403
352.5	2.5969	933.16	92.358	152.02	15.779
355.0	2.7386	913.77	88.126	164.27	16.208
357.5	2.8864	892.88	83.838	178.00	16.702
360.0	3.0405	870.11	79.456	193.58	17.280
362.5	3.2012	844.89	74.924	211.59	17.974
365.0	3.3690	816.28	70.150	232.90	18.832
367.5	3.5443	782.64	64.976	259.15	19.946
370.0	3.7278	740.32	59.052	293.90	21.527
372.5	3.9205	677.22	51.233	349.09	24.320

TABLE A2. Viscosity of R134a in the single phase regions

Temperature	210 K		220 K		230 K	
Pressure (MPa)	Density (kg m^{-3})	Viscosity (μPa s)	Density (kg m^{-3})	Viscosity (μPa s)	Density (kg m^{-3})	Viscosity (μPa s)
0.01	0.58902	8.2880	0.56142	8.6886	0.53643	9.0888
0.05	1483.12	701.61	1455.24	582.24	1426.80	492.14
0.10	1483.21	701.98	1455.34	582.55	1426.91	492.40
0.15	1483.30	702.35	1455.44	582.85	1427.02	492.66
0.20	1483.39	702.71	1455.54	583.15	1427.13	492.91
0.25	1483.48	703.08	1455.64	583.45	1427.24	493.17
0.30	1483.57	703.45	1455.74	583.75	1427.35	493.43
0.35	1483.66	703.82	1455.84	584.05	1427.46	493.68
0.40	1483.75	704.19	1455.94	584.35	1427.58	493.94
0.50	1483.92	704.93	1456.14	584.96	1427.80	494.45
0.60	1484.10	705.67	1456.33	585.56	1428.02	494.97
0.80	1484.46	707.15	1456.73	586.77	1428.46	496.00
1.00	1484.81	708.63	1457.12	587.98	1428.90	497.03
1.50	1485.69	712.35	1458.10	591.02	1429.99	499.60
2.00	1486.56	716.08	1459.07	594.06	1431.08	502.19
2.50	1487.43	719.83	1460.04	597.12	1432.15	504.78
3.00	1488.29	723.59	1461.00	600.19	1433.22	507.38
3.50	1489.15	727.38	1461.95	603.26	1434.28	509.98
4.00	1490.01	731.18	1462.90	606.35	1435.34	512.59
5.00	1491.70	738.83	1464.77	612.56	1437.42	517.83
6.00	1493.38	746.55	1466.62	618.82	1439.48	523.11
8.00	1496.67	762.21	1470.26	631.48	1443.50	533.75
10.00	1499.90	778.18	1473.81	644.34	1447.43	544.52
15.00	1507.69	819.52	1482.36	677.47	1456.81	572.12
20.00	1515.12	863.08	1490.46	712.13	1465.66	600.79
25.00	1522.23	909.10	1498.18	748.50	1474.05	630.68
30.00	1529.05	957.82	1505.56	786.77	1482.04	661.95
35.00	1535.61	1009.53	1512.63	827.13	1489.66	694.74
40.00	1541.93	1064.49	1519.42	869.80	1496.96	729.21
45.00	1548.03	1123.03	1525.96	914.98	1503.97	765.54
50.00	1553.94	1185.47	1532.28	962.93	1510.71	803.89
55.00	1559.66	1252.18	1538.38	1013.88	1517.22	844.46

Temperature	240 K		250 K		260 K	
Pressure (MPa)	Density (kg m^{-3})	Viscosity (μPa s)	Density (kg m^{-3})	Viscosity (μPa s)	Density (kg m^{-3})	Viscosity (μPa s)
0.01	0.51364	9.4884	0.49277	9.8874	0.47356	10.285
0.05	2.6171	9.4756	2.5034	9.8758	2.4003	10.275
0.10	1397.78	422.06	5.1144	9.8618	4.8874	10.263
0.15	1397.91	422.29	1367.96	365.78	7.4723	10.251
0.20	1398.03	422.51	1368.10	365.99	1337.13	319.46
0.25	1398.16	422.74	1368.24	366.20	1337.29	319.66
0.30	1398.28	422.97	1368.38	366.40	1337.46	319.85
0.35	1398.41	423.19	1368.52	366.61	1337.62	320.04
0.40	1398.53	423.42	1368.67	366.81	1337.78	320.23
0.50	1398.78	423.87	1368.95	367.22	1338.10	320.61
0.60	1399.03	424.32	1369.23	367.63	1338.43	320.99
0.80	1399.53	425.23	1369.79	368.45	1339.07	321.76
1.00	1400.02	426.13	1370.35	369.27	1339.71	322.52
1.50	1401.25	428.40	1371.74	371.32	1341.30	324.43
2.00	1402.47	430.67	1373.12	373.38	1342.86	326.33
2.50	1403.68	432.94	1374.48	375.43	1344.41	328.24
3.00	1404.88	435.22	1375.83	377.48	1345.94	330.14
3.50	1406.06	437.50	1377.17	379.54	1347.46	332.03
4.00	1407.24	439.78	1378.49	381.59	1348.96	333.93
5.00	1409.57	444.36	1381.10	385.71	1351.90	337.72
6.00	1411.86	448.95	1383.67	389.83	1354.79	341.51
8.00	1416.33	458.20	1388.66	398.10	1360.39	349.09
10.00	1420.67	467.53	1393.48	406.41	1365.77	356.68
15.00	1431.01	491.30	1404.90	427.47	1378.42	375.79
20.00	1440.69	515.82	1415.52	449.03	1390.09	395.21

TABLE A2. Viscosity of R134a in the single phase regions—Continued

Temperature	240 K		250 K		260 K	
Pressure (MPa)	Density ($kg\ m^{-3}$)	Viscosity ($\mu Pa\ s$)	Density ($kg\ m^{-3}$)	Viscosity ($\mu Pa\ s$)	Density ($kg\ m^{-3}$)	Viscosity ($\mu Pa\ s$)
25.00	1449.82	541.22	1425.46	471.23	1400.94	415.07
30.00	1458.47	567.63	1434.83	494.18	1411.10	435.49
35.00	1466.69	595.18	1443.70	518.00	1420.67	456.59
40.00	1474.54	624.00	1452.13	542.80	1429.73	478.46
45.00	1482.04	654.23	1460.17	568.71	1438.33	501.20
50.00	1489.24	686.00	1467.85	595.82	1446.54	524.93
55.00	1496.17	719.47	1475.23	624.27	1454.38	549.73
Temperature	270 K		273 K		280 K	
Pressure (MPa)	Density ($kg\ m^{-3}$)	Viscosity ($\mu Pa\ s$)	Density ($kg\ m^{-3}$)	Viscosity ($\mu Pa\ s$)	Density ($kg\ m^{-3}$)	Viscosity ($\mu Pa\ s$)
0.01	0.45582	10.683	0.45076	10.802	0.43938	11.079
0.05	2.3061	10.673	2.2794	10.793	2.2195	11.071
0.10	4.6834	10.662	4.6260	10.782	4.4982	11.061
0.15	7.1389	10.652	7.0461	10.772	6.8408	11.052
0.20	9.6816	10.642	9.5475	10.763	9.2531	11.044
0.25	12.322	10.634	12.140	10.755	11.742	11.036
0.30	1305.26	280.69	1295.31	270.10	14.315	11.030
0.35	1305.45	280.87	1295.50	270.28	16.982	11.025
0.40	1305.63	281.05	1295.70	270.46	1271.91	247.46
0.50	1306.01	281.42	1296.09	270.82	1272.35	247.82
0.60	1306.38	281.78	1296.48	271.18	1272.78	248.17
0.80	1307.12	282.51	1297.26	271.90	1273.65	248.88
1.00	1307.86	283.24	1298.03	272.62	1274.52	249.59
1.50	1309.69	285.05	1299.95	274.42	1276.65	251.36
2.00	1311.49	286.86	1301.83	276.21	1278.75	253.11
2.50	1313.27	288.67	1303.69	277.99	1280.81	254.86
3.00	1315.03	290.47	1305.52	279.77	1282.84	256.60
3.50	1316.76	292.26	1307.32	281.54	1284.84	258.34
4.00	1318.46	294.05	1309.10	283.31	1286.81	260.06
5.00	1321.82	297.63	1312.59	286.83	1290.66	263.49
6.00	1325.09	301.19	1315.99	290.34	1294.39	266.91
8.00	1331.40	308.28	1322.55	297.32	1301.57	273.67
10.00	1337.44	315.36	1328.81	304.28	1308.39	280.39
15.00	1351.52	333.05	1343.35	321.62	1324.11	297.05
20.00	1364.36	350.89	1356.58	339.07	1338.30	313.71
25.00	1376.22	369.01	1368.76	356.76	1351.28	330.53
30.00	1387.25	387.55	1380.07	374.83	1363.27	347.64
35.00	1397.59	406.61	1390.65	393.38	1374.44	365.14
40.00	1407.32	426.29	1400.60	412.51	1384.90	383.15
45.00	1416.53	446.68	1410.00	432.31	1394.76	401.74
50.00	1425.29	467.87	1418.92	452.87	1404.10	421.00
55.00	1433.63	489.95	1427.42	474.28	1412.97	441.02
Temperature	290 K		298 K		300 K	
Pressure (MPa)	Density ($kg\ m^{-3}$)	Viscosity ($\mu Pa\ s$)	Density ($kg\ m^{-3}$)	Viscosity ($\mu Pa\ s$)	Density ($kg\ m^{-3}$)	Viscosity ($\mu Pa\ s$)
0.01	0.42410	11.474	0.41262	11.789	0.40985	11.867
0.05	2.1396	11.467	2.0799	11.782	2.0655	11.861
0.10	4.3289	11.458	4.2033	11.775	4.1731	11.854
0.15	6.5711	11.450	6.3726	11.768	6.3251	11.848
0.20	8.8703	11.444	8.5909	11.762	8.5244	11.842
0.25	11.231	11.438	10.861	11.757	10.774	11.837
0.30	13.658	11.432	13.188	11.753	13.077	11.833
0.35	16.157	11.428	15.574	11.750	15.437	11.830
0.40	18.735	11.425	18.025	11.747	17.859	11.828
0.50	24.163	11.422	23.143	11.746	22.909	11.827
0.60	1237.20	218.84	28.597	11.750	28.275	11.831
0.80	1238.24	219.55	1208.11	198.50	1200.28	193.51
1.00	1239.27	220.26	1209.31	199.21	1201.53	194.24

TABLE A2. Viscosity of R134a in the single phase regions—Continued

Temperature	290 K		298 K		300 K	
Pressure (MPa)	Density (kg m^{-3})	Viscosity (μPa s)	Density (kg m^{-3})	Viscosity (μPa s)	Density (kg m^{-3})	Viscosity (μPa s)
1.50	1241.80	222.01	1212.26	200.99	1204.60	196.02
2.00	1244.27	223.75	1215.13	202.75	1207.58	197.79
2.50	1246.70	225.48	1217.93	204.49	1210.50	199.54
3.00	1249.09	227.20	1220.67	206.22	1213.34	201.27
3.50	1251.42	228.91	1223.35	207.92	1216.12	202.98
4.00	1253.72	230.60	1225.97	209.62	1218.83	204.68
5.00	1258.18	233.96	1231.06	212.97	1224.09	208.03
6.00	1262.50	237.29	1235.94	216.27	1229.13	211.33
8.00	1270.72	243.85	1245.18	222.75	1238.66	217.80
10.00	1278.47	250.33	1253.81	229.10	1247.53	224.14
15.00	1296.13	266.26	1273.26	244.62	1267.47	239.57
20.00	1311.85	282.04	1290.37	259.87	1284.95	254.70
25.00	1326.08	297.86	1305.72	275.06	1300.60	269.75
30.00	1339.13	313.86	1319.69	290.35	1314.81	284.89
35.00	1351.20	330.17	1332.54	305.88	1327.87	300.24
40.00	1362.45	346.87	1344.47	321.73	1339.97	315.91
45.00	1373.01	364.06	1355.61	338.02	1351.26	331.99
50.00	1382.96	381.82	1366.08	354.80	1361.87	348.56
55.00	1392.38	400.23	1375.98	372.18	1371.88	365.70
Temperature	310 K		320 K		330 K	
Pressure (MPa)	Density (kg m^{-3})	Viscosity (μPa s)	Density (kg m^{-3})	Viscosity (μPa s)	Density (kg m^{-3})	Viscosity (μPa s)
0.01	0.39654	12.260	0.38408	12.650	0.37238	13.039
0.05	1.9966	12.254	1.9324	12.646	1.8723	13.036
0.10	4.0291	12.248	3.8955	12.641	3.7711	13.032
0.15	6.0993	12.243	5.8908	12.637	5.6975	13.029
0.20	8.2090	12.239	7.9195	12.634	7.6525	13.027
0.25	10.360	12.235	9.9834	12.631	9.6372	13.026
0.30	12.556	12.232	12.084	12.629	11.653	13.025
0.35	14.798	12.230	14.223	12.629	13.701	13.025
0.40	17.090	12.229	16.403	12.628	15.783	13.026
0.50	21.835	12.230	20.893	12.631	20.054	13.030
0.60	26.821	12.235	25.574	12.638	24.480	13.038
0.80	37.684	12.262	35.611	12.665	33.862	13.067
1.00	1160.44	170.74	46.786	12.718	44.097	13.117
1.50	1164.27	172.61	1119.57	151.11	75.467	13.384
2.00	1167.97	174.45	1124.33	153.09	1074.80	133.08
2.50	1171.55	176.26	1128.89	155.03	1080.92	135.24
3.00	1175.02	178.05	1133.27	156.92	1086.69	137.32
3.50	1178.40	179.81	1137.48	158.77	1092.17	139.34
4.00	1181.67	181.54	1141.54	160.58	1097.38	141.30
5.00	1187.97	184.95	1149.25	164.12	1107.12	145.07
6.00	1193.95	188.28	1156.49	167.55	1116.09	148.68
8.00	1205.12	194.76	1169.77	174.14	1132.21	155.50
10.00	1215.38	201.04	1181.79	180.46	1146.46	161.94
15.00	1238.05	216.17	1207.74	195.45	1176.43	176.96
20.00	1257.56	230.82	1229.60	209.77	1201.03	191.06
25.00	1274.79	245.28	1248.63	223.77	1222.08	204.71
30.00	1290.29	259.73	1265.55	237.68	1240.58	218.18
35.00	1304.42	274.33	1280.85	251.66	1257.16	231.65
40.00	1317.44	289.17	1294.86	265.82	1272.22	245.25
45.00	1329.53	304.35	1307.79	280.27	1286.05	259.08
50.00	1340.83	319.96	1319.83	295.09	1298.87	273.25
55.00	1351.45	336.07	1331.10	310.36	1310.82	287.82

TABLE A2. Viscosity of R134a in the single phase regions—Continued

Temperature	340 K		350 K		360 K	
Pressure (MPa)	Density ($kg\ m^{-3}$)	Viscosity ($\mu Pa\ s$)	Density ($kg\ m^{-3}$)	Viscosity ($\mu Pa\ s$)	Density ($kg\ m^{-3}$)	Viscosity ($\mu Pa\ s$)
0.01	0.36138	13.426	0.35101	13.811	0.34122	14.194
0.05	1.8159	13.423	1.7629	13.809	1.7130	14.193
0.10	3.6548	13.421	3.5459	13.808	3.4436	14.193
0.15	5.5176	13.419	5.3495	13.808	5.1922	14.194
0.20	7.4049	13.418	7.1745	13.808	6.9593	14.195
0.25	9.3177	13.418	9.0213	13.808	8.7453	14.197
0.30	11.257	13.418	10.891	13.810	10.551	14.199
0.35	13.223	13.420	12.784	13.812	12.377	14.202
0.40	15.218	13.421	14.700	13.815	14.223	14.206
0.50	19.298	13.428	18.610	13.823	17.980	14.216
0.60	23.505	13.437	22.626	13.834	21.827	14.228
0.80	32.347	13.468	31.010	13.867	29.814	14.264
1.00	41.854	13.517	39.927	13.916	38.238	14.314
1.50	69.696	13.752	65.275	14.132	61.679	14.518
2.00	1015.59	113.63	97.518	14.562	89.974	14.888
2.50	1024.59	116.23	952.49	96.835	126.89	15.560
3.00	1032.82	118.67	966.22	100.09	186.15	17.057
3.50	1040.41	120.98	978.08	103.01	893.69	83.910
4.00	1047.48	123.20	988.61	105.70	913.12	87.801
5.00	1060.34	127.36	1006.80	110.56	942.47	94.108
6.00	1071.84	131.26	1022.28	114.95	964.99	99.341
8.00	1091.87	138.48	1047.98	122.77	999.46	108.12
10.00	1109.04	145.14	1069.07	129.78	1026.00	115.62
15.00	1143.97	160.33	1110.22	145.28	1075.01	131.61
20.00	1171.77	174.31	1141.78	159.24	1110.99	145.61
25.00	1195.11	187.70	1167.71	172.43	1139.85	158.66
30.00	1215.36	200.81	1189.88	185.25	1164.15	171.24
35.00	1233.33	213.86	1209.36	197.94	1185.25	183.62
40.00	1249.53	226.98	1226.78	210.66	1203.98	196.00
45.00	1264.32	240.30	1242.59	223.54	1220.86	208.48
50.00	1277.95	253.91	1257.09	236.66	1236.27	221.19
55.00	1290.62	267.88	1270.50	250.13	1250.46	234.21

Temperature	370 K		380 K		390 K	
Pressure (MPa)	Density ($kg\ m^{-3}$)	Viscosity ($\mu Pa\ s$)	Density ($kg\ m^{-3}$)	Viscosity ($\mu Pa\ s$)	Density ($kg\ m^{-3}$)	Viscosity ($\mu Pa\ s$)
0.01	0.33197	14.574	0.32320	14.952	0.31489	15.328
0.05	1.6659	14.574	1.6214	14.954	1.5792	15.330
0.10	3.3473	14.576	3.2564	14.956	3.1705	15.333
0.15	5.0444	14.577	4.9052	14.958	4.7740	15.337
0.20	6.7577	14.579	6.5683	14.962	6.3899	15.341
0.25	8.4875	14.582	8.2458	14.966	8.0186	15.346
0.30	10.234	14.586	9.9380	14.970	9.6602	15.352
0.35	11.998	14.590	11.645	14.975	11.315	15.358
0.40	13.780	14.595	13.368	14.981	12.983	15.365
0.50	17.399	14.606	16.861	14.994	16.361	15.380
0.60	21.095	14.621	20.421	15.011	19.796	15.398
0.80	28.734	14.659	27.750	15.051	26.847	15.441
1.00	36.735	14.710	35.384	15.104	34.156	15.496
1.50	58.647	14.908	56.028	15.299	53.725	15.690
2.00	84.188	15.240	79.494	15.606	75.549	15.980
2.50	115.31	15.783	106.92	16.074	100.34	16.400
3.00	156.44	16.717	140.37	16.791	129.22	16.999
3.50	223.40	18.736	184.27	17.961	164.12	17.869
4.00	787.42	65.647	251.91	20.255	208.72	19.202
5.00	857.42	76.919	707.99	54.909	377.18	26.544
6.00	895.34	83.934	802.55	67.790	655.55	48.918
8.00	944.72	94.290	881.39	81.055	805.96	68.208
10.00	979.11	102.51	927.53	90.285	870.28	78.869
15.00	1038.20	119.15	999.64	107.77	959.25	97.367
20.00	1079.37	133.25	1046.90	122.02	1013.58	111.80

TABLE A2. Viscosity of R134a in the single phase regions—Continued

Temperature	370 K		380 K		390 K	
Pressure (MPa)	Density (kg m^{-3})	Viscosity (μPa s)	Density (kg m^{-3})	Viscosity (μPa s)	Density (kg m^{-3})	Viscosity (μPa s)
25.00	1111.53	146.20	1082.75	134.89	1053.53	124.61
30.00	1138.15	158.57	1111.92	147.09	1085.47	136.65
35.00	1161.02	170.69	1136.67	158.97	1112.23	148.31
40.00	1181.14	182.75	1158.26	170.75	1135.38	159.83
45.00	1199.15	194.90	1177.47	182.59	1155.83	171.39
50.00	1215.51	207.24	1194.82	194.59	1174.20	183.09
55.00	1230.51	219.86	1210.66	206.86	1190.91	195.04

Temperature	400 K		410 K		420 K	
Pressure (MPa)	Density (kg m^{-3})	Viscosity (μPa s)	Density (kg m^{-3})	Viscosity (μPa s)	Density (kg m^{-3})	Viscosity (μPa s)
0.01	0.30700	15.701	0.29949	16.071	0.29235	16.438
0.05	1.5392	15.704	1.5012	16.075	1.4651	16.443
0.10	3.0891	15.708	3.0120	16.080	2.9386	16.449
0.15	4.6498	15.713	4.5323	16.086	4.4208	16.456
0.20	6.2216	15.718	6.0624	16.093	5.9116	16.464
0.25	7.8045	15.725	7.6024	16.100	7.4111	16.472
0.30	9.3989	15.731	9.1525	16.107	8.9196	16.481
0.35	11.005	15.738	10.713	16.115	10.437	16.490
0.40	12.622	15.746	12.283	16.124	11.964	16.499
0.50	15.894	15.763	15.456	16.143	15.045	16.520
0.60	19.215	15.783	18.673	16.164	18.164	16.543
0.80	26.014	15.829	25.241	16.214	24.522	16.596
1.00	33.034	15.886	32.001	16.273	31.045	16.658
1.50	51.673	16.080	49.824	16.469	48.144	16.856
2.00	72.150	16.359	69.171	16.741	66.522	17.123
2.50	94.936	16.745	90.360	17.103	86.400	17.469
3.00	120.70	17.270	113.82	17.577	108.06	17.906
3.50	150.44	17.981	140.11	18.190	131.85	18.452
4.00	185.71	18.962	170.04	18.984	158.22	19.131
5.00	285.05	22.504	245.62	21.423	221.02	21.033
6.00	458.75	31.914	354.01	26.079	302.05	24.084
8.00	714.53	55.730	609.73	44.439	511.21	36.157
10.00	806.57	68.235	736.55	58.485	662.77	49.907
15.00	917.03	87.889	873.12	79.288	827.87	71.536
20.00	979.46	102.51	944.64	94.069	909.28	86.429
25.00	1023.93	115.26	994.01	106.76	963.85	99.027
30.00	1058.83	127.14	1032.05	118.48	1005.20	110.58
35.00	1087.73	138.59	1063.19	129.72	1038.67	121.62
40.00	1112.50	149.88	1089.66	140.78	1066.88	132.46
45.00	1134.25	161.17	1112.74	151.82	1091.34	143.26
50.00	1153.68	172.59	1133.27	162.98	1112.98	154.17
55.00	1171.28	184.24	1151.78	174.36	1132.42	165.28

Temperature	430 K		440 K		450 K	
Pressure (MPa)	Density (kg m^{-3})	Viscosity (μPa s)	Density (kg m^{-3})	Viscosity (μPa s)	Density (kg m^{-3})	Viscosity (μPa s)
0.01	0.28554	16.802	0.27903	17.162	0.27282	17.520
0.05	1.4307	16.807	1.3979	17.169	1.3665	17.527
0.10	2.8689	16.815	2.8025	17.178	2.7391	17.537
0.15	4.3148	16.823	4.2139	17.187	4.1178	17.547
0.20	5.7684	16.832	5.6323	17.197	5.5027	17.558
0.25	7.2298	16.841	7.0576	17.207	6.8938	17.569
0.30	8.6991	16.851	8.4900	17.218	8.2912	17.581
0.35	10.176	16.861	9.9295	17.229	9.6950	17.593
0.40	11.662	16.871	11.376	17.240	11.105	17.606
0.50	14.657	16.894	14.291	17.265	13.945	17.632
0.60	17.687	16.919	17.236	17.292	16.811	17.661
0.80	23.849	16.975	23.218	17.351	22.624	17.723
1.00	30.156	17.040	29.326	17.418	28.549	17.794

TABLE A2. Viscosity of R134a in the single phase regions—Continued

Temperature	430 K		440 K		450 K	
Pressure (MPa)	Density ($kg\ m^{-3}$)	Viscosity ($\mu Pa\ s$)	Density ($kg\ m^{-3}$)	Viscosity ($\mu Pa\ s$)	Density ($kg\ m^{-3}$)	Viscosity ($\mu Pa\ s$)
1.50	46.606	17.242	45.190	17.625	43.878	18.005
2.00	64.140	17.506	61.980	17.887	60.005	18.268
2.50	82.916	17.839	79.810	18.212	77.013	18.586
3.00	103.12	18.250	98.812	18.603	94.993	18.963
3.50	124.99	18.749	119.13	19.067	114.05	19.400
4.00	148.77	19.349	140.94	19.612	134.28	19.903
5.00	203.38	20.931	189.75	20.983	178.72	21.125
6.00	269.64	23.217	246.66	22.826	229.11	22.682
8.00	436.95	31.317	385.00	28.677	347.58	27.197
10.00	590.89	42.909	527.11	37.709	474.41	34.119
15.00	781.88	64.617	736.01	58.516	691.24	53.212
20.00	873.59	79.536	837.87	73.341	802.45	67.796
25.00	933.58	92.009	903.35	85.650	873.30	79.897
30.00	978.35	103.38	951.59	96.820	925.00	90.847
35.00	1014.21	114.22	989.87	107.44	965.71	101.24
40.00	1044.21	124.82	1021.68	117.83	999.34	111.40
45.00	1070.07	135.40	1048.96	128.17	1028.03	121.51
50.00	1092.84	146.07	1072.87	138.60	1053.09	131.72
55.00	1113.22	156.93	1094.20	149.23	1075.36	142.12

12. References

[1] A. S. Teja and P. A. Thurner, Chem. Eng. Commun. **49**, 79 (1986).
[2] B. Willman and A. S. Teja, Chem. Eng. J. **37**, 65 (1988).
[3] K. J. Okeson and R. L. Rowley, Int. J. Thermophys. **12**, 119 (1991).
[4] G. Scalabrin and M. Grigiante, Proceedings 13th Symposium Thermophysical Properties, Boulder, CO, 22–27 June 1997.
[5] G. Cristofoli, M. Grigiante, and G. Scalabrin, High Temp.-High Press. **33**, 83 (2001).
[6] G. Scalabrin, G. Cristofoli, and M. Grigiante, Int. J. Energy Research **26**, 1 (2002).
[7] J. F. Ely and H. J. M. Hanley, Ind. Eng. Chem. Fundam. **20**, 323 (1981).
[8] M. L. Huber and J. F. Ely, Fluid Phase Equilibria **80**, 239 (1992).
[9] S. A. Klein, M. O. McLinden, and A. Laesecke, Int. J. Refrig. **30**, 2089 (1997).
[10] M. O. McLinden, S. A. Klein, E. W. Lemmon, and A. P. Peskin, *NIST Standard Reference Database 23, Version 6.0* REFPROP, 1998.
[11] R. Krauss, J. Luettmer-Strathmann, J. V. Sengers, and K. Stephan, Int. J. Thermophys. **14**, 951 (1993).
[12] A. Laesecke, R. Krauss, K. Stephan, and W. Wagner, J. Phys. Chem. Ref. Data **19**, 1089 (1990).
[13] G. Scalabrin, C. Corbetti, and G. Cristofoli, Int. J. Thermophys. **22**, 1383 (2001).
[14] G. Cristofoli, L. Piazza, and G. Scalabrin, Fluid Phase Equilibria **199**, 223 (2002).
[15] G. Scalabrin, L. Piazza, and V. Vesovic, High Temp.-High Press. **34**, 457 (2002).
[16] G. Scalabrin and G. Cristofoli, Int. J. Refrig. **26**, 302 (2003).
[17] G. Scalabrin and G. Cristofoli, Int. J. Thermophys. **24**, 1241 (2003).
[18] G. Scalabrin, G. Cristofoli, and D. Richon, Fluid Phase Equilibria **199**, 265 (2002).
[19] G. Scalabrin, G. Cristofoli, and D. Richon, Fluid Phase Equilibria **199**, 281 (2002).
[20] U. Setzmann and W. Wagner, Int. J. Thermophys. **10**, 1103 (1989).
[21] R. Tillner-Roth and H. D. Baehr, J. Phys. Chem. Ref. Data **23**, 657 (1994).
[22] P. J. Mohr and B. N. Taylor, Rev. Mod. Phys. **72**, 351 (2000).
[23] P. Becker, H. Bettin, H.-U. Danzebrink, M. Glaser, U. Kuetgens, A. Nicolaus, D. Schiel, P. De Bievre, S. Valkiers, and P. Taylor, Metrologia **40**, 271 (2003).
[24] M. J. Assael, J. H. Dymond, and S. K. Polimatidou, Int. J. Thermophys. **15**, 591 (1994).
[25] D. E. Diller, A. S. Aragon, and A. Laesecke, Fluid Phase Equilibria **88**, 251 (1993).
[26] T. Okubo, T. Hasuo, and A. Nagashima, Int. J. Thermophys. **13**, 931 (1992).
[27] C. M. B. P. Oliveira and W. A. Wakeham, Int. J. Thermophys. **14**, 33 (1993).
[28] A. A. H. Padua, J. M. N. Fareleira, J. C. G. Calado, and W. A. Wakeham, J. Chem. Eng. Data **41**, 731 (1996).
[29] G. Y. Ruvinskij, G. K. Lavrenchenko, S. V. Iljushenko, and V. V. Kanaev, Int. J. Refrig. **15**, 386 (1992).
[30] L. Z. Han, M. S. Zhu, X. Y. Li, and D. Luo, J. Chem. Eng. Data **40**, 650 (1995).
[31] R. Heide, DKV-Tagungsbericht, Leipzig **23**, 225 (1996).
[32] A. Kumagai and S. Takahashi, Int. J. Thermophys. **12**, 105 (1991).
[33] A. Laesecke, T. O. D. Luddecke, R. F. Hafer, and D. J. Morris, Int. J. Thermophys. **20**, 401 (1999).
[34] A. A. H. Padua, J. M. N. A Fareleira, J. C. G Calado, and W. A. Wakeham, Int. J. Thermophys. **17**, 781 (1996).
[35] D. Ripple and O. Matar, J. Chem. Eng. Data **38**, 560 (1993).
[36] N. G. Sagaidakova, V. A. Rykov, and T.N. Tsuranova, Kholod. Tekh. **5**, 59 (1990).
[37] I. R. Shankland, R. S. Basu, and D. P. Wilson, Proceedings Meeting International Institute of Refrigeration, Commissions B1, B2, E1, E2, Purdue University, West Lafayette, IN, 18–21 July 1988, Vol. II, p. 305.
[38] M. J. Assael and S. K. Polimatidou, Int. J. Thermophys. **18**, 353 (1997).
[39] D. C. Dowdell and G. P. Matthews, J. Chem. Soc. Faraday. Trans. **89**, 3545 (1993).
[40] F. Mayinger, *Messung der Viskosität an Neuen Arbeitsstoffen und Deren Gemischen in Dampfformigen und Überkritischen Zustand* (DFG-Forschungsvorhaben, Abschlußbericht, 1991).
[41] H. Nabizadeh and F. Mayinger, High Temp.-High Press. **24**, 221 (1992).
[42] M. F. Pasekov and E. E. Ustyuzhanin, Teplofiz. Vys. Temp. **32**, 630 (1994).
[43] B. Schramm, J. Hauck, and L. Kern, Ber. Bunsenges. Phys. Chem. **96**, 745 (1992).
[44] N. Shibasaki-Kitakawa, M. Takahashi, and C. Yokoyama, Int. J. Thermophys. **19**, 1285 (1998).
[45] J. Wilhelm and E. Vogel, Fluid Phase Equilibria **125**, 257 (1996).

[46] C. M. B. P. Oliveira and W. A. Wakeham, Int. J. Thermophys. **20**, 365 (1999).
[47] G. A. Olchowy and J. V. Sengers, Phys. Rev. Lett. **61**, 15 (1988).
[48] G. A. Olchowy and J. V. Sengers, Int. J. Thermophys. **10**, 417 (1989).
[49] J. V. Sengers, Int. J. Thermophys. **6**, 203 (1985).
[50] M. L. Huber, A. Laesecke, and R. Perkins, Ind. Eng. Chem. Res. **42**, 3163 (2003).
[51] M. L. Huber and M. O. McLinden, Proceedings International Refrigeration Conference, Purdue University, West Lafayette, IN, 14–17 July 1992, Vol. II, p. 453.
[52] E. W. Lemmon and R. T. Jacobsen, Int. J. Thermophys. **25**, 21 (2004).
[53] E. Vogel, C. Küchenmeister, E. Bich, and A. Laesecke, J. Phys. Chem. Ref. Data **27**, 947 (1998).
[54] D. G. Friend and J. C. Rainwater, Chem. Phys. Lett. **107**, 590 (1984).
[55] J. C. Rainwater and D. G. Friend, Phys. Rev. A **36**, 4062 (1987).